

# **Geospatial Analysis of Wildfire in Los Angeles – 2025**

**A PROJECT REPORT**

*Submitted by*

**ARRCHANA T**

**EDHISHA S P**

**JEBASTIN J**

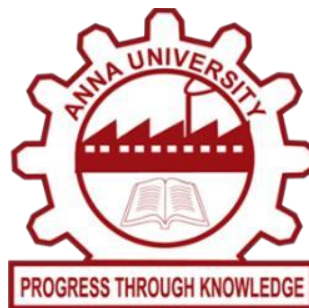
**MOHAMED IMTHIYAZ S**

*in partial fulfillment of the award of the degree  
of*

**BACHELOR OF ENGINEERING**

**IN**

**GEOINFORMATICS ENGINEERING**



**DEPARTMENT OF CIVIL ENGINEERING  
ANNA UNIVERSITY REGIONAL CAMPUS TIRUNELVELI  
ANNA UNIVERSITY: CHENNAI 600 025  
MAY 2024**

# **ANNA UNIVERSITY: CHENNAI 600 025**

## **BONAFIDE CERTIFICATE**

Certified that this project report “**Geospatial Analysis of Wildfire in Los Angeles – 2025**” is the Bonafide work of “**ARRCHANAA T (950021135007), EDHISHA S P(950021135016), JEBASTIN J(950021135024), MOHAMED IMTHIYAZ S(950021135029)**” who carried out the project work under my supervision.

**Dr. S. ADISHKUMAR, M.E., Ph.D.,  
HEAD OF THE DEPARTMENT,  
Assistant professor,  
Department of Civil Engineering,  
Anna University Regional Campus,  
Tirunelveli – 627 007.**

**Dr.J. Thirumal,M.E., Ph.D.,  
SUPERVISOR,  
Assistant Professor,  
Department of Civil Engineering,  
Anna University Regional Campus,  
Tirunelveli – 627 007.**

Submitted for the VIVA–VOCE Examination held on \_\_\_\_\_.

**INTERNAL EXAMINER**

**EXTERNAL EXAMINER**



## **ACKNOWLEDGEMENT**

First and foremost, we immensely thank God Almighty for showering his grace and blessings for the successful completion of this project.

We deeply thankful to **Dr.C.Lakshumanan** Head of the Department of Remote sensing, for the assistance during this project work.

We extend my heartfelt gratitude to **D.J.Saravanavel**, Professor, Department of Remote Sensing, Bharathidasan University for their invaluable guidance, unwavering support, and insightful feedback throughout the course of this project. Their expertise and encouragement have been instrumental in shaping the direction and quality of this work.

We would like to thank **Dr. Shenbaga Vinayaga Moorthi M.E., Ph.D.**, the dean of the Anna University Regional Campus Tirunelveli.

We wholeheartedly thank **Dr.S. Adishkumar, M.E., Ph.D.**, Head of the Department of Civil Engineering, Anna University Regional Campus, Tirunelveli.

We are grateful to **Dr. J.THIRUMAL , M.E., Ph.D.**, Assistant Professor, Department of Civil Engineering, Anna University Regional Campus Tirunelveli for his guidance, knowledge sharing and valuable suggestions to complete the project work.

We have deep gratitude towards **Mrs.G. Devi, MTech.**, our Project coordinator, for her excellent support, valuable suggestions and constant support to complete the project.

Finally, we would like to thank our beloved parents and friends for their unwavering support and encouragement needed throughout the enriching project.

## **ABSTRACT**

Wildfires pose a serious threat to ecosystems, infrastructure, and human safety, particularly in highly urbanized and ecologically sensitive regions such as Los Angeles, California. This study employs Remote Sensing and Geographic Information System (GIS)-based analysis to assess wildfire susceptibility using a multi-criteria evaluation approach. Key biophysical and anthropogenic factors such as land cover, vegetation index (NDVI), slope, aspect, temperature, precipitation, and proximity to roads and settlements were analysed to evaluate fire risk. High-resolution satellite imagery was used to derive burn indices and vegetation stress indicators, while historical fire data aided in model validation and accuracy assessment. A wildfire risk map was generated for the study area, classifying zones into high, moderate, and low susceptibility. Results showed that 35% of the area is highly susceptible, 28% moderately susceptible, and 37% less susceptible to wildfires. Critical infrastructure and densely populated zones were mapped against high-risk areas to identify priority zones for emergency planning and resource allocation. The findings underscore the importance of integrating spatial technologies into wildfire risk management, offering valuable insights for urban planners, environmental managers, and disaster response agencies. This research highlights the potential of geospatial techniques in supporting proactive strategies for wildfire prevention, mitigation, and resilience building in fire-prone regions

## **TABLE OF CONTENT**

<b>CHAPTER NO.</b>	<b>TITLE</b>	<b>PAGE NO.</b>
	<b>ACKNOWLEDGEMENT</b> <b>ABSTRACT</b> <b>TABLE OF CONTENTS</b> <b>LIST OF FIGURES</b> <b>LIST OF TABLES</b> <b>ABBREVIATIONS</b>	IV
1	<b><u>INTRODUCTION</u></b>  1.1 General 1.2 Type of forest fire 1.3 Background 1.4 Historical forest fire in California 1.5 Forest fire policies in US 1.6 Forest fire mitigation project in US 1.7 Aim and objective 1.8 Need of study 1.9 Conclusion	1
2	<b><u>REVIEW OF LITERATURE</u></b>  2.1 General 2.2 Literature review 2.3 Conclusion	10
3	<b><u>STUDY AREA AND ITS DESCRIPTION</u></b>  3.1 General 3.2 Geographical location of study area	14

	3.3 Physiography 3.4 Basemap 3.5 Conclusion	
	<b><u>MATERIAL AND METHODOLOGY</u></b>	
4	4.1 General 4.2 Dataset 4.3 Methodology 4.4 Software use 4.5 Conclusion	19
	<b><u>DRIVING FACTOR OF FORESTFIRE</u></b>	
5	<p>5.1 Physiographic factor</p> <p>5.1.1 Elevation 5.1.2 Slope 5.1.3 Aspect 5.1.4 Topographical roughness index 5.1.5 Land use and landcover 5.1.6 Normalized burn index 5.1.7 Differential normalized burn index (dNBR) 5.1.8 Normalized difference vegetation index</p> <p>5.2 Damage Assessment</p> <p>5.3 Climatic factor</p> <p>5.3.1 Land surface temperature</p>	32
		46
		47

	5.3.2 Wind direction 5.3.3 Wind speed	
	<b>5.4 Anthropogenic factor</b>	52
	5.4.1 Proximity of road 5.4.1 Proximity of settlements	
	<b>5.5 GIS BASED AHP</b>	54
	5.5.1 Analytical hierarchy process (AHP) method 5.5.2 Pair wise comparison matrix 5.5.3 Normalized pair wise comparison matrix 5.5.4 Calculating consistency 5.5.5 Random consistency index 5.5.6 Checking consistency 5.5.7 Parameter reclassification	
	<b>6.1 Risk zone Map</b>	64
	<b>7.1 Validation Map</b>	66
7	<b>CONCLUSION</b>	67

## **LIST OF FIGURES**

<b>FIGURE NO.</b>	<b>TITLE</b>	<b>PAGE NO.</b>
3.1	STUDY AREA	16
3.2	BASEMAP	17
4.1	METHODOLOGY	27
5.1	ELEVATION	33
5.2	SLOPE	34
5.3	ASPECT	35
5.4	TOPOGRAPHICAL ROUGHNESS INDEX	36
5.5	LANDUSE LANDCOVER	37
5.6	NBR (PRE)	38
5.7	NBR(POST)	39
5.8	dNBR	40
5.9	NDVI (2019)	42
5.10	NDVI (2020)	42
5.11	NDVI (2021)	43
5.12	NDVI (2022)	43
5.13	NDVI (2023)	44
5.14	NDVI (2024)	44
5.15 (a) & (b)	NDVI (PRE AND POST)	45
5.16	DAMAGE ASSESSMENT	46

5.17 (a) & (b)	LST	48,49
5.18	WIND DIRECTION	50
5.19	WIND SPEED	51
5.20	PROXIMITY OF ROAD	53
5.21	PROXIMITY OF SETTLEMENT	54
6.1	RISK ZONE MAP	63
7.1	VALIDATION MAP	63

## **LIST OF TABLES**

<b>TABLE</b>	<b>TITLE</b>	<b>PAGE NO.</b>
1	Forest fire mitigation project in the united states	7
2	Dataset	19
3	Saaty preference table	56
4	Pair wise comparison matrix	57
5	Normalized pair wise comparison matrix	59
6	Random consistency Index	61
7	Calculating consistency	63
8	Wildfire risk area	65

## ABBREVIATIONS

ArcGIS	Aeronautical Reconnaissance Coverage Geographical Information System
GIS	Geographic Information System
DEM	Digital Elevation Model
DEM	Digital Elevation Model
OSM	Open street map
NOAA weather data	National oceanic and atmospheric administration.
USGS	United States Geological Survey
NASA FIRMS	Fire Information for Resource Management System data
AHP	Analytical Hierarchy Process
NDVI	Normalized Difference Vegetation Index
NBR	Normalized Burn Ratio
dNBR	Differenced Normalized Burn Ratio
OLI	Operational Land Imager
TIRS	Thermal Infrared Sensor
LST	Land surface temperature
TRI	Topographic Ruggedness Index
LULC	Land use and Land cover

# **CHAPTER 1**

## **INTRODUCTION**

### **1.1 GENERAL**

Fires are a major natural disturbance of forest ecosystems, influencing ecological processes, biodiversity, forest structures, and landscape patterns. Depending on the fire regime, forest fires can be a threat to people's lives and cause economic and environmental damages. Large intensive fires have huge impacts on the physical health, as the exposure to smoke is associated with an increased risk of respiratory cardiovascular diseases, among others. Experiencing the threat to personal safety and the loss of properties and belongings can have long-lasting consequences on mental health, causing depression, post traumatic stress disorder, and anxiety. Moreover, forest fires generate considerable economic losses due to damaged infrastructure and settlements, health costs, and the disruption of supply chains. Depending on characteristics of fires (i.e., size, type, and intensity), there are numerous environmental impacts and related ecosystem services, including carbon emissions, soil degradation, desertification, loss of forests, and biodiversity decline. Furthermore, forest fires in mountainous regions endanger protection forests, leading to a higher vulnerability to natural hazards like avalanches and landslides, and they reduce cultural ecosystem services such as recreational and aesthetic experiences.

The occurrence of forest fires is associated with various environmental and anthropogenic factors such as weather conditions, vegetation characteristics, and human activities. Regions characterized by dry climatic conditions have always been prone to forest fires, located, for example, around the Mediterranean in Europe, in western North America, and Australia.

## **1.2 TYPE OF FOREST FIRE**

**Surface fire:** A forest fire is typically a surface fire that spreads across the forest floor as senescent leaves and twigs, dried grasses, and other detritus.

**Underground Fire:** Underground fires are low-intensity fires that destroy organic material beneath the forest floor and the forest floor's surface litter. On top of the mineral soil, a thick layer of organic material is found in the majority of dense woods. Typically, these flames start when such materials are consumed and spread underground for a few metres. This type of fire spreads very quietly, making it difficult to detect and control. Muck fires are also known as these types of fires as they can burn for months and destroy the soil's vegetation.

**Ground fire:** The fires occur in the organic substrates, such as the subsurface duff layers under forest stands, the tundra or taiga in the Arctic, or the organic soils in swampy or boggy areas. A smouldering underground fire can occasionally turn into a ground fire. It's difficult to tell the difference between underground and ground fires. This fire burns the herbaceous growth on forest floors as well as the decaying organic layers, i.e., the fire burns the herbaceous growth on forest floors as well as the decaying organic layers. Smouldering combustion can cause severe harm when ground fires burn below the surface. Surface fires often spark ground fires. Ground fires can destroy vegetation completely.

**Crown fire:** A crown fire is defined as a fire that burns the tops of trees and plants and is frequently generated by a surface fire. Because of the burning resinous substance shed by burning logs, these fires are especially dangerous in pine forests. Because warm air moves quickly uphill, spreading flames along the way, a fire that starts downhill on a steep slope is likely to spread uphill early. It's less likely for a fire to spread downhill if it starts uphill.

**Firestorms:** The most common forest fires are firestorms, which are large fires that spread quickly. Heat increases when the fire burns, causing heat to rise and air to rush in, causing

the fire to spread. More air creates a fire that spins violently like a tornado, with flames shooting from its base and embers on top, igniting little fires all around it. Inside these storms, flame temperatures can exceed 2,000 degrees Fahrenheit.

## **1.3 BACKGROUND**

One of the most wildfire-prone regions in the United States is Los Angeles, California. The city and its surrounding counties frequently experience large-scale forest fires, particularly during the late summer and fall seasons. Los Angeles is uniquely vulnerable due to its semi-arid climate, topography, and the prevalence of Santa Ana winds, which can rapidly accelerate the spread of fire across vast areas. Additionally, the wildland-urban interface (WUI)—zones where human development meets undeveloped wildland vegetation—has expanded significantly in recent decades, placing more lives and properties at risk.

Los Angeles has witnessed some of the most destructive wildfires in the United States, leading to significant ecological loss, displacement of communities, health hazards due to air pollution, and billions of dollars in damages. The proximity of urban developments to fire-prone wildlands further increases the region's vulnerability, making wildfires not only a natural disaster but also a complex urban planning and public safety challenge.

In recent years, climate change has intensified the frequency, duration, and severity of wildfires in Southern California. Rising temperatures, prolonged droughts, and reduced moisture in vegetation contribute to an environment where fires can ignite more easily and spread more aggressively. These challenges underscore the urgent need for effective systems to detect, predict, and manage wildfires before they escalate into large-scale disasters.

## **1.4 HISTORICAL FOREST FIRE IN CALIFORNIA (U.S.A)**

### **Early 20th Century:**

#### **1910 Great Fire:**

This event, also known as the Big Burn, was a devastating series of fires that burned across a vast area, impacting forests and settlements throughout California and the Pacific Northwest.

#### **1918 Cloquet Fire:**

While not solely a California fire, this devastating blaze in Minnesota, sparked by a railroad, burned over 250,000 acres and killed hundreds, serving as a stark reminder of the destructive power of wildfires.

#### **1932 Matilija Fire:**

This fire, in the Santa Barbara National Forest, burned nearly 220,000 acres.

#### **1933 Griffith Park Fire:**

This fire in Los Angeles tragically claimed the lives of 25 firefighters, highlighting the dangers of fire suppression efforts.

### **Mid-20th Century:**

#### **1953 Rattlesnake Fire:**

This fire on the Mendocino National Forest led to the creation of the first federal task force on wildland fire safety, setting the stage for modern fire management practices.

## **Late 20th and Early 21st Century:**

### **2003 Cedar Fire:**

This fire in San Diego County burned over 273,000 acres, destroyed thousands of structures, and resulted in numerous fatalities, marking a significant turning point in understanding the impact of wildfires on communities.

### **2007 Witch Fire:**

This fire, fueled by strong winds, burned over 197,000 acres and caused extensive damage, particularly in San Diego County.

## **Recent Fires:**

### **2017 Thomas Fire:**

This fire, which burned across Ventura and Santa Barbara counties, became one of the largest in California's history, causing significant damage and destruction.

### **2017 Tubbs Fire:**

This fire in Sonoma and Napa counties, part of the broader North Bay fires, was particularly destructive, claiming lives and destroying numerous homes.

### **2018 Camp Fire:**

This devastating fire in Butte County caused unprecedented destruction, claiming numerous lives and leaving Paradise in ruins, highlighting the vulnerability of communities to wildfires.

### **2018 Carr Fire:**

This fire in Shasta and Trinity counties burned over 229,000 acres and caused significant property damage, further underscoring the growing threat of wildfires in the state.

### **2020 August Complex Fire:**

This fire, the largest in California history, burned over a million acres, causing widespread destruction and loss of life, especially in the Mendocino National Forest.

### **2020 SCU Lightning Complex and LNU Lightning Complex:**

These fires, part of the broader 2020 fire season, burned vast areas, including parts of the Bay Area, demonstrating the widespread impact of wildfires across California.

### **2021 Dixie Fire:**

This fire, one of the largest in California history, burned over 963,000 acres and caused significant damage to communities in Butte, Plumas, Lassen, and Tehama counties.

### **2025 January Fires:**

A series of fires in Southern California, including the Eaton and Palisades fires, caused extensive damage and loss of life, highlighting the continued threat of wildfires even during winter months.

## **1.5 Forest Fire Policies in the United States**

### **1.5.1 FEDERAL WILDFIRE POLICIES**

1 National Fire Plan (NFP) – 2000

2 Healthy Forests Restoration Act (HFRA) – 2003

3 National Cohesive Wildland Fire Management Strategy (2014)

4 Infrastructure Investment and Jobs Act (2021)

### **1.5.2 STATE-LEVEL POLICIES**

1 California Fire Prevention Laws and Regulations

2 SB 901 (2018) Wildfire Prevention and Utility Regulation

3 California Wildfire and Forest Resilience Action Plan (2021)

### **1.5.3 LOCAL AND COMMUNITY POLICIES**

1 Community Wildfire Protection Plans (CWPPs)

2 Firewise USA® Program

### **1.5.4 EMERGENCY AND DISASTER POLICIES**

1 Stafford Act (1988)

2 Federal Land Assistance, Management and Enhancement Act (FLAME Act, 2009)

## **1.6 FOREST FIRE MITIGATION PROJECT IN THE UNITED STATES**

<b>Project Name</b>	<b>Lead Agency</b>	<b>Scope</b>	<b>Focus Area</b>	<b>Status</b>
Wildfire Crisis Strategy	USFS	National	Fuel reduction	Ongoing (2022–2032)
CalVTP	CAL FIRE	CA	Vegetation treatment	Active
CWDG	USDA FS	National	Community resilience	Ongoing

Firewise USA®	NFPA	Local	Home safety & outreach	Expanding
FIRIS	Cal OES	CA	Real-time intelligence	Active in LA
LANDFIRE	USGS/USFS	National	Data-driven planning	Ongoing
LAC Fuel Program	LA Co. FD	Local	Brush clearance	Ongoing
TREX	NGOs + USFS	National	Prescribed fire	Periodic

TABLE -1 mitigation project in the united states

## **1.7 AIM AND OBJECTIVE**

The aim of this study is to analyze burn coverage, wildfire damage assessment, and develop a forest fire risk map for the 2025 Los Angeles wildfire using Remote Sensing and GIS.

- To analyze the burn coverage of Los Angeles using indices such as NBR, and dNBR .
- To create a damage assessment map, methods such as NDVI analysis, Building damage assesment, and the integration of anthropogenic factors like distance from roads and settlements are used
- To visualize forest fire risk assessment mapping using AHP (Analytic Hierarchy Process) analysis.

- To validating the results with NASA FIRMS data.

## **1.8 NEED OF STUDY**

1.Burn Assessment - Helping to quantify wildfire-affected areas.

2 .Damage Assessment Mapping – Supports rapid evaluation of fire impact on infrastructure, vegetation

3. Forest Fire Risk Assessment Mapping – Identifies high-risk zones to enhance fire prevention, preparedness, and resource allocation for wildfire management.

## **1.9 CONCLUSION**

From this chapter,an overview of the forest fire, its classification, the Historical events, Policies and mitigation project, and the objective of the study are explained

# **CHAPTER 2**

## **REVIEW OF LITERATURE**

### **2.1 GENERAL**

This chapter discusses the literature that have been reviewed in order to conduct the entire study

### **2.2 REVIEW OF LITERATURE**

**Kilian Gerberding, Uta Schirpke.,(2025)** on his research goal is to assess current and future forest fire risk across the European Alps with the assistance of geospatial modelling in the context of climate change. More advanced technologies including GIS, remote sensing, and machine learning make wildfire forecasting, mapping, and risk analysis better, while Multi-Criteria Decision Analysis and AHP improve fire susceptibility modeling. Human activities and global warming are worsening fires, and effective risk assessment and data-driven fire management require sophisticated GIS, machine learning, and remote sensing

**Oishi Bhattacharya, Suman Sinha et al., (2024)** The research uses GIS and remote sensing to map forest fire risk zones in Pauri Garhwal, Uttarakhand, considering climatic, biotic, and topographic factors. It then uses AHP to identify areas of wildfire risk based on these variables. Fire danger maps are calibrated against NASA FIRMS data, and sensitivity analysis is performed to evaluate wildfire susceptibility. The AHP method determines 4-10% low risk and 30-40% moderate risk.

**S.Latha.,(2023)**on her study demonstrates the effectiveness of satellite imagery and GIS-based analysis in assessing forest fire risk. Techniques like NDVI, NBR, and LST mapping aid in identifying fire-risk areas. Multi-criteria decision analysis using Weighted Overlay Analysis in ArcGIS categorizes fire-prone areas. The research reveals that over 51% of Nilgiris District is extremely vulnerable to forest fires, necessitating extensive fire management practices, remote sensing, GIS-based mapping, and public participation.

**Edmond Pasho et al., (2022)** The study was conducted in National Park "Dajti Mountain" (NPDM), Albania, located 5 km northeast of Tirana, covering diverse forested regions. The study used Landsat 8 satellite imagery to analyze pre- and post-fire conditions, applying indices like dNBR, NBR2, NDVI, and EVI for burn severity and vegetation recovery assessment. Field data from Composite Burn Index (CBI) plots were collected to validate remote sensing results. The study found that dNBR and dNBR2 indices effectively mapped burned areas, with dNBR achieving 91.7% accuracy in fire severity assessment. NDVI and EVI analysis showed significant post-fire vegetation recovery,

**Mohamed Elhag, Nese Yilmaz et al.,(2020)**The study was conducted on Thasos Island, Greece, a fire-prone region in the northern Aegean Sea. The study used Landsat-8 satellite images to analyze pre- and post-fire conditions, along with Normalized Difference Vegetation Index (NDVI) for vegetation assessment .The study found that Principal Component Analysis (PCA) combined with NDVI differencing effectively mapped burned areas, achieving 84.61% accuracy in fire detection

**Hassan Abedi Gheshlaghi.,(2019)**on his study area develop a model for forest fire risk mapping in Noshahar country, country,Northern Iran by using ANP tool.ANP incorporate factors like physiographic and climate.Model validated using MODIS fire data, achieving an AUC of 0.783, indicating good predictive accuracy.57.45% of the study area falls under high and very high-risk categories, highlighting the need for preventive strategies and better forest management.

**Dr. Veera Narayana Balabathina et al.,(2014)**The study uses IRS LISS-III satellite imagery and GIS-based modeling to identify forest fire-prone areas in Guntur District, Andhra Pradesh. It processes vegetation Indices and topographic analysis to allocate weightage and create a susceptibility map. The results show the effectiveness of GIS, remote sensing, and risk modeling in identifying wildfire-risk areas, justifying improved fire prevention, forest management, and policy planning to minimize wildfire risks.

**Laxmi Kant Sharma,Shruti Kanga et al.,(2012)**To study fire risk zone in Taradevi forest range Himachal Pradesh using MCDA.To analysis environmental and climate factor by using IRS-P6-LISS-3and topological maps. The study apply the fuzzy AHP to refine fire risk mapping ,ensuring a more precise classification of high risk zone.The study developed a GIS-based MCDA model for mapping wildfire risk, reducing

**Jaehoon Jung,Joon heo et al., (2012)**This study analyzes the wildfire risk zone map of Kolli Hills,Tamil nadu Some elements like slope,roads, and distance from settlements are universaly and suitable for the assessment of wildfire hazards.The Analytic Hierarchy Process (AHP) is an hierarchical process used to compare and provide weights for multiple criteria with the aim of making sound decision-making.The research verifies that GIS-based analysis AHP accurately identify fireprone locations inKolliHills, and humanactivities within settlements and along roads enhance fire risk; Indian expert group's model (90.38% accuracy) indicates the necessity for standardized global fire risk assessment

**Matthias M. Boer, Craig Macfarlane et al.,(2008)**A study conducted in south-western Australia on the Perth Hills fires in 2005, which destroyed 27,700 ha of jarrah forest, used Landsat Thematic Mapper satellite imagery to examine vegetation change and

Leaf Area Index (LAI) estimates. The severity of the fire was evaluated using the Differenced Normalized Burn Ratio ( $\Delta$ NBR) and confirmed with fire history data from the Department of Environment and Conservation, Western Australia. The study found that change detection of LAI accurately mapped burned regions and fire severity.

## **2.3 CONCLUSION**

From the literature Forest fire risk is increasing globally due to climate change, with temperature, humidity, and human activity being major contributing factors. Geospatial tools, remote sensing, and machine learning have been effectively used to map fire-prone areas and predict future risks. These approaches support better forest management, early warning systems, and climate resilience planning

# **CHAPTER 3**

## **STUDY AREA AND ITS DISCRIPTION**

### **3.1 GENERAL**

This chapter deals with the study area and its description

### **3.2 GEOGRAPHICAL LOCATION OF STUDY AREA**

Los Angeles is a city in Southern California, situated on the east coast of the Pacific Ocean. It is part of Los Angeles County and the Greater Los Angeles Metropolitan Area, and is surrounded by a variety of natural landforms that significantly impact its climate, ecosystem, and fire danger profile. The city is situated at the juncture of coastal plains, mountain ranges, and desert basins, with the Santa Monica Mountains and San Gabriel Mountains ringing it to the north and east, and the Los Angeles Basin extending south towards the Long Beach and Orange County line. The city's proximity to ecologically sensitive wildland-urban interface areas, such as Griffith Park, Topanga Canyon, Malibu, and the Angeles National Forest, increases its exposure to wildfires. The city's Mediterranean climate of hot, dry summers and cool, wet winters has increased its susceptibility to forest fires due to severe droughts, lower annual precipitation, and higher temperatures. Changes in seasonal weather patterns, including heat waves late in the season, have raised the frequency and intensity of wildfire activity throughout the county. The geographical character of Los Angeles is crucial to understanding how wildfires initiate, propagate, and affect both natural environments and human infrastructure, making it a focus for research on wildfire behavior and mitigation efforts.

### **3.3 PHYSIOGRAPHY**

Los Angeles' physiography is a complex blend of coastal plains, mountain ranges, valleys, and upland plateaus, which significantly impacts its climate, vegetation distribution, land use, and wildfire behavior. The city is located within the Transverse Ranges Province, a unique geological region in Southern California, where mountain ranges run east-west. These ranges include the Santa Monica Mountains, San Gabriel Mountains, and Verdugo Mountains, which contribute to sharp elevation changes. The Los Angeles Basin, a broad coastal lowland in the southwestern part of the city, is drained by rivers like the Los Angeles River and San Gabriel River, forming alluvial valleys and floodplains that are now densely urbanized. The basin is underlain by sedimentary deposits and is seismically active due to multiple faults. The Santa Monica Mountains, an east-west trending range, are covered with flammable vegetation and the San Gabriel Mountains dominate the skyline with rugged topography, deep canyons, and sparse vegetation. The region is highly susceptible to erosion, landslides, and flash floods, particularly after wildfires remove vegetation. The wildland-urban interface (WUI) is particularly pronounced in areas like Malibu, Topanga, Bel-Air, and Altadena, influenced by physiographic factors such as rugged slopes, narrow canyons, and limited road access. In summary, Los Angeles' physiographic setting is a key factor in understanding its ecological diversity, urban planning challenges, and wildfire vulnerability. The combination of rugged mountains, arid hills, and densely populated lowlands intensifies natural hazards like forest fires.

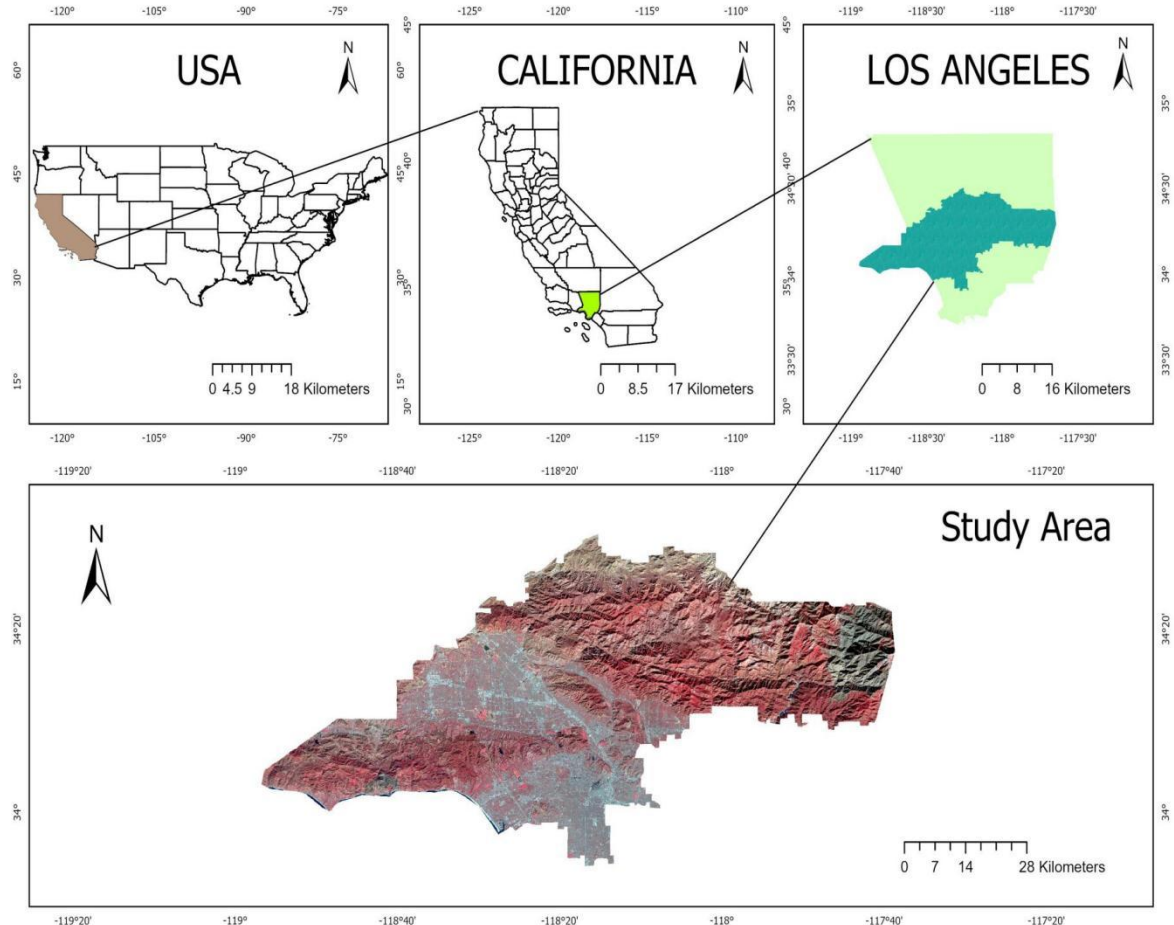


Figure 3.1 Study area

### **3.4 BASE MAP**

The study area's foundational map was created utilizing USGS topview toposheet and have been update using the satellite imagery. Various geographic features, including road, water body, predominant places, mountains, forest, metro lines were digitally mapped. Notable mountains and forest identified in the study area include **Santa Monica mountain , San Gabriel mountain and Angeles national forest** among others. Most of the area reserve forest reflecting the rich natural environment among the settlements. The road has been designed by the Federal Highway Administration (FHWA) as U.S 101 as

Oregon Coast Highway, Olympic Highway is a major north–south highway that traverses the states of California, Oregon, and Washington on the West Coast of the United States. The Los Angeles River historically known as **West River** its is a major river in Los Angeles County.

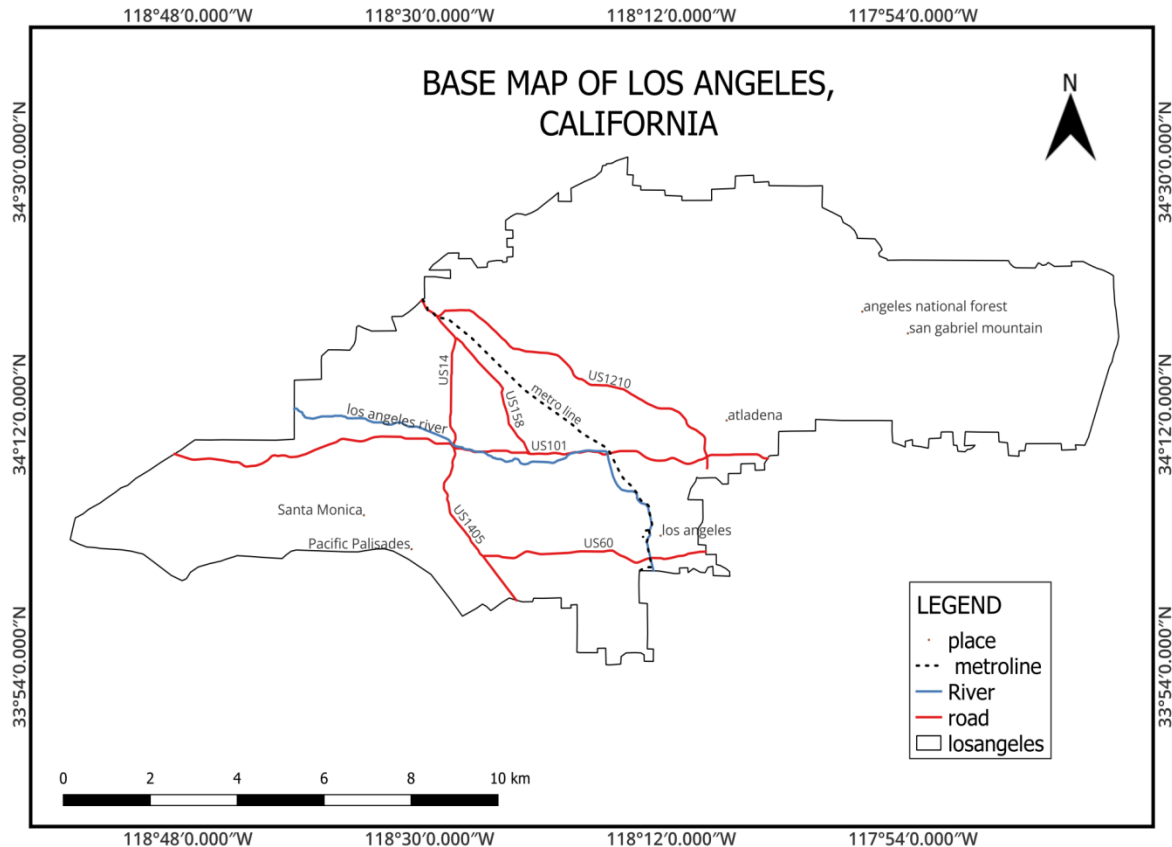


Figure- 3.2 Basemap

### **3.5 CONCLUSION**

Los Angeles' diverse geography and physiography, including mountains, basins, and wildland-urban interfaces, make it highly vulnerable to wildfires. Its Mediterranean climate, combined with drought and dense vegetation, increases fire risk. The base map highlights key features like forests, rivers, and transport networks, providing a solid foundation for wildfire analysis and mitigation planning.

# **CHAPTER 4**

## **MATERIAL AND METHODOLOGY**

### **4.1 GENERAL**

The assessment of forest fire risk zones involves integrating multiple data sources, including satellite data from Landsat 8/9, Sentinel-2 imagery, meteorological data from the NASA Power dataset, topographic features from the SRTM DEM, anthropogenic data from Open Street Map, and fire hotspot data from NASA FIRMS (MODIS). These data are used to derive indices like NBR, NDVI, NBI, and LST, extract Land Use Land Cover information, and validate active fire locations using fire hotspot data from NASA FIRMS. The Analytical Hierarchy Process (AHP) is applied to assign appropriate weights to each thematic layer, which are then used within GIS to generate a forest fire risk zone map. The resulting forest fire risk zones are validated using fire hotspot data from NASA FIRMS to ensure accuracy.

### **4.2 DATASET**

<b><u>S.NO</u></b>	<b><u>DATASET</u></b>	<b><u>SOURCE</u></b>	<b><u>PURPOSE</u></b>
1	Landsat 8/9 (OLI/TIRS)	USGS	Burn severity (NBR)
2	Landsat 8/9 (OLI/TIRS)	USGS	vegetation analysis (NDVI)

3	Landsat 9	USGS	Land use and Land cover
4	NOAA Weather Data	NOAA data viewer	Wind speed
6	NOAA Weather Data	NOAA data viewer	Wind direction
7	DEM (SRTM)	USGS	Terrain analysis for fire spread modeling
8	LANDSAT	NASA FIRMS	To identify the active fire places
9	OSM	HOT osm	To develop a proximity map and for damage assessment

Table -2 Data set

## 4.3 DATA DISCRIPTION

### 4.3.1 DEM

A Digital Elevation Model (DEM) is a 3-Dimentional representation of the Topography of a land surface or terrain. DEMs are often used in GIS and are the most common basis for digitally produced relief maps. In the study, we used SRTM (Shuttle Radar Topography Mission) DEM with a 30m spatial resolution to perform slope, flow accumulation, SPI, TWI, TRI, relief, lineament and lineament density. The data was downloaded from the USGS Earth Explorer.

#### **4.4.2 LANDSAT 8/9**

Landsat 8 and 9 are Earth observation satellites that carry two main instruments: the Operational Land Imager (OLI) and the Thermal Infrared Sensor (TIRS). OLI captures imagery in nine spectral bands, including visible, near-infrared, and shortwave infrared, with a 30-meter spatial resolution (except the 15-meter panchromatic band). TIRS collects thermal infrared data in two bands at a 100-meter resolution, resampled to 30 meters for consistency. These sensors enable monitoring of land use, vegetation health, water bodies, and urban development. The satellites have a 16-day repeat cycle, providing global coverage for environmental and resource management. Data from Landsat 8/9 is radiometrically and geometrically corrected, ensuring high accuracy and comparability. The mission supports climate research, disaster response, and agricultural planning. Landsat data is freely available to the public, making it one of the most widely used sources for remote sensing analysis. Together, Landsat 8 and 9 ensure continuity of the Landsat program's decades-long Earth observation legacy.

#### **4.4.3 NOAA Weather Data**

NOAA (National Oceanic and Atmospheric Administration) provides comprehensive weather data through various platforms, satellites, and observational systems. It collects data on temperature, precipitation, wind, humidity, and atmospheric pressure from ground stations, buoys, aircraft, and weather balloons. NOAA's satellite systems, such as GOES and JPSS, offer real-time and forecast meteorological data, including cloud cover and storm tracking. The National Weather Service (NWS), a branch of NOAA, distributes forecasts, warnings, and alerts for public safety. NOAA also gathers oceanographic and climate data, supporting marine navigation and long-term climate studies. This data is crucial for weather prediction models, disaster preparedness, and environmental monitoring. NOAA maintains several public data portals, like NOAA NCEI and NOAA Weather and Climate Toolkit, to ensure accessibility. Its datasets support

sectors including aviation, agriculture, emergency management, and research. NOAA's commitment to open data sharing promotes science-based decision-making. Overall, NOAA plays a central role in the U.S. and global weather and climate information infrastructure.

#### **4.4.4 NASA FIRMS**

NASA FIRMS (Fire Information for Resource Management System) are two distinct but complementary satellite-based Earth observation systems managed by NASA. Landsat, a joint program by NASA and USGS, provides high-resolution multispectral imagery useful for long-term land cover and land use monitoring, operating since the 1970s. It captures detailed data on vegetation, water bodies, urban growth, and environmental change. NASA FIRMS, on the other hand, delivers near real-time active fire and thermal anomaly data using moderate-resolution sensors like MODIS and VIIRS. FIRMS data is used for wildfire detection, disaster response, and air quality monitoring. While Landsat offers finer spatial resolution (30m) with slower revisit times (16 days), FIRMS provides frequent updates (as often as every few hours) but at coarser resolution. Together, these datasets support wildfire risk assessment, burn area mapping, and ecosystem monitoring. Both are freely accessible and widely used in environmental management and research. Combining Landsat and FIRMS allows for both rapid fire alerts and detailed post-fire analysis.

#### **4.4.5 OpenStreetMap**

OpenStreetMap (OSM) is a collaborative, open-source project that provides free and editable geographic data of the world. It is created and maintained by a global community of volunteers who collect data using GPS devices, aerial imagery, and local knowledge. OSM includes detailed information on roads, buildings, land use, waterways, points of interest, and more. Unlike commercial mapping services, OSM data

is openly licensed under the Open Database License (ODbL), allowing unrestricted use, modification, and sharing. The data is widely used in web mapping, humanitarian efforts, navigation, and geographic information systems (GIS). OSM supports rapid mapping in disaster-affected areas, often coordinated through organizations like the Humanitarian OpenStreetMap Team (HOT). It is updated continuously, making it highly dynamic and responsive to real-world changes. OSM data can be accessed via APIs or downloaded in various formats for offline analysis. Its open nature encourages innovation and customization for diverse applications. Overall, OSM serves as a powerful, community-driven alternative to proprietary geographic datasets.

## **4.4 SOFTWARE USE**

GIS software are computer-based programs and tools that allows the user to visualize, analyze, interpret and store the geographic datasets. The software that has been used for the study are,

1. ArcGIS
2. ArcGIS PRO
3. QGIS
4. ENVI
5. Google Earth Engine

### **1. ArcGIS**

ArcGIS is a Desktop software developed by ESRI which can be used primarily to view, edit, create, and analyze geospatial datasets. ArcMAP 10.8 has been used in particular, which is a part of the ArcGIS desktop suite.

ArcMAP is the former main component of ESRI's ArcGIS suite of geospatial processing programs. ArcMap allows the user to explore data within a data set, symbolize

features accordingly, and create maps. The ArcMap interface has two main sections, including the table of contents on the left and the data frames which display the map. Items in the table of contents correspond with the layers on the map.

## **2. ArcGIS PRO**

ArcGIS Pro is a professional desktop GIS software developed by Esri for advanced spatial analysis, data visualization, and map creation. It offers a modern 64-bit architecture with an intuitive ribbon-based interface and seamless integration with ArcGIS Online. ArcGIS Pro supports 2D and 3D data, enabling complex geospatial modeling and real-time data processing. It provides tools for geoprocessing, remote sensing, and data management across various formats and databases. Widely used in government, academia, and industry, ArcGIS Pro is a powerful platform for solving real-world geographic problems.

## **3. QGIS**

QGIS (Quantum GIS) is a free and open-source Geographic Information System used for viewing, editing, analyzing, and visualizing geospatial data. It supports a wide range of file formats and databases, including shapefiles, GeoTIFFs, and PostGIS. QGIS offers powerful tools for map creation, spatial analysis, and geoprocessing through a user-friendly interface and plugins. It is widely used in research, urban planning, environmental management, and education. With active community support and regular updates, QGIS is a reliable alternative to commercial GIS software.

## **4. ENVI**

ENVI (Environment for Visualizing Images) is a software platform for processing and analyzing geospatial imagery, particularly remote sensing data. It offers

powerful tools for image enhancement, classification, and change detection, often used with data from satellites, UAVs, and aerial surveys. ENVI supports a wide range of formats, including multispectral, hyperspectral, and radar data. The software provides advanced analysis capabilities, such as spectral unmixing and object-based classification, with an intuitive user interface. ENVI is commonly used in fields like environmental monitoring, agriculture, and defense for geospatial analysis and decision-making.

## **5. Google Earth Engine**

Google Earth Engine is a cloud-based platform for geospatial analysis, offering access to a vast repository of satellite imagery and environmental data. It allows users to analyze large datasets at scale, leveraging powerful computational resources without the need for extensive local processing. With its comprehensive data catalog, including Landsat, Sentinel, and MODIS, users can perform tasks like environmental monitoring, deforestation detection, and climate change analysis. Google Earth Engine uses JavaScript and Python APIs for script-based analysis and visualization. It is widely used by researchers, NGOs, and government agencies for scientific studies and resource management.

## **4.5 METHODOOGY**

To assess forest fire risk zones, multiple data sources are integrated. Satellite data from Landsat 8/9 is used to derive indices such as NBR (Normalized Burn Ratio), NDVI (Normalized Difference Vegetation Index), NBI (Normalized Built-up Index), and LST (Land Surface Temperature). Additionally, Sentinel-2 imagery is used to extract Land Use Land Cover (LULC) information. Meteorological data is obtained from the NASA Power dataset, which includes parameters such as wind speed, temperature, humidity, and wind direction. Topographic features are derived from the SRTM DEM, which provides data on slope, aspect, elevation, and terrain ruggedness index (TRI). Anthropogenic data, including

roads and settlements, is collected from OpenStreetMap (OSM). Fire hotspot data is acquired from NASA FIRMS (MODIS) to identify and validate active fire locations. These datasets are used to perform an assessment of weight on thematic layers that influence forest fire risk. The Analytical Hierarchy Process (AHP) is applied to assign appropriate weights to each thematic layer. These criteria weights are then used within GIS to generate a forest fire risk zone map. Finally, the resulting forest fire risk zones are validated using the fire hotspot data from NASA FIRMS to ensure accuracy.

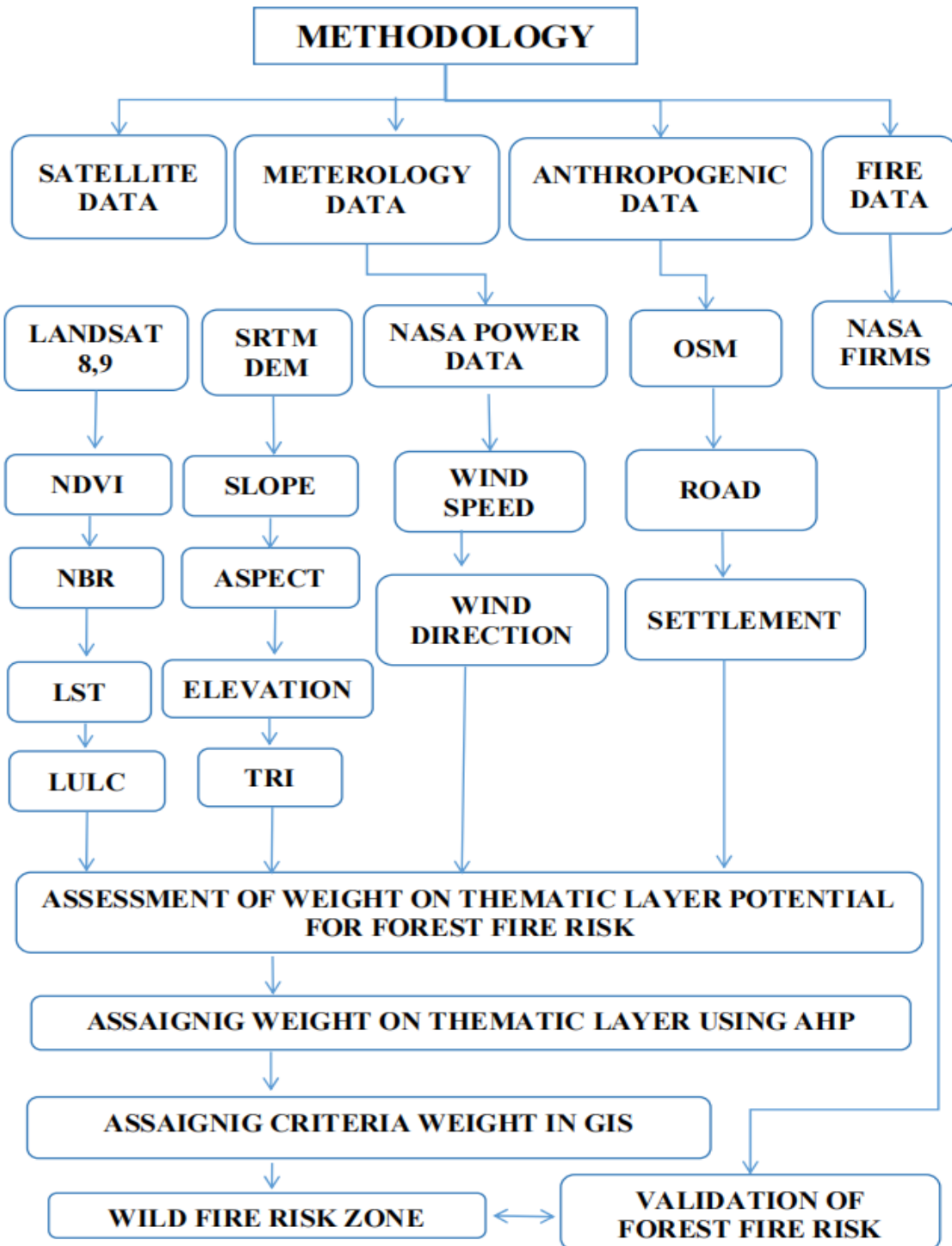


Figure -4.1 Methodology

## **ELEVATION:**

In Geographic Information Systems (GIS), elevation refers to the height of a geographic location or feature above or below a reference plane, usually mean sea level. It's a crucial component of understanding terrain and is used for various analyses, including calculating slopes, viewsheds, and for creating topographic maps.

## **SLOPE:**

Slope is a key aspect of terrain analysis in GIS, providing insights into the steepness of the landscape. It's calculated as the maximum rate of change in elevation between a location and its surroundings.

## **ASPECT:**

In Geographic Information Systems (GIS), aspect refers to the compass direction a slope faces. It's a crucial parameter in terrain analysis, representing the horizontal direction of the slope's steepness. Essentially, it's the direction the slope is facing, typically measured clockwise in degrees from 0 to 360, with 0 degrees representing north.

## **TOPOGRAPHICAL ROUGHNESS INDEX**

In Geographic Information Systems (GIS), the Topographic Roughness Index (TRI) is a measure of how uneven or rugged a terrain is. It quantifies the variation in elevation between a central grid cell and its surrounding cells. This index is a valuable tool for analyzing digital elevation models (DEMs) and understanding local surface spatial variability, often used in geomorphology, ecology, and land use planning.

## **NORMALIZED VEGETATION INDEX**

NDVI is a numerical index that uses the visible and near-infrared bands of the electromagnetic spectrum to analyze remote sensing measurements and assess whether the target being observed contains live green vegetation.

Formula:

$$\text{NDVI} = (\text{NIR} + \text{RED}) / (\text{NIR} - \text{RED})$$

## **NORMALIZED BURN RATIO**

NBR is a spectral index used primarily to identify burned areas and assess fire severity. It compares near-infrared (NIR) and shortwave infrared (SWIR) reflectance from satellite imagery.

Formula:

$$\text{NBR} = (\text{NIR} + \text{SWIR}) / (\text{NIR} - \text{SWIR})$$

Where ,

NIR = Near-Infrared reflectance (e.g., Landsat Band 5)

SWIR = Shortwave Infrared reflectance (e.g., Landsat Band 7)

## **DIFFERENCED NORMALIZED BURN RATIO**

dNBR is a commonly used index to assess the severity of wildfires by comparing the Normalized Burn Ratio (NBR) before and after a fire. It highlights the differences in the landscape caused by the fire, helping to evaluate the extent and severity of the burn.

Formula:

$$dNBR = (NBR_{prefire}) - (NBR_{postfire})$$

Where:

NBR\_pre-fire is the Normalized Burn Ratio calculated from satellite data before the fire.

NBR\_post-fire is the Normalized Burn Ratio calculated from satellite data after the fire

.

## **LAND SURFACE TEMPERATURE**

LST - Land Surface Temperature (LST) is the radiative skin temperature of the land derived from solar radiation. LST, the skin temperature of the ground, is identified as a significant variable of micro climate and radiation transfer within the atmosphere. For the current study, Landsat 9 with the Thermal bands can facilitate LST calculation by the formula:

$$LST = BT/I + W * (BT/p) * \ln(e)$$

Where,

LST - Land Surface Temperature, e - Emissivity, BT - Brightness Temperature, p – 14380, W-Wavelength of emitted radiance (11.5 $\mu$ m).

## **LANDUSE LANDCOVER**

Land Use and Land Cover (LULC) refers to the classification of the Earth's surface based on human activities (land use) and natural physical features (land cover). Land cover includes forests, water bodies, and bare soil, while land use represents areas used for agriculture, urban development, or industry. LULC data is vital for urban planning, environmental management, and climate change studies. It is typically derived from satellite imagery through classification techniques in GIS and remote sensing. Monitoring LULC changes helps in assessing human impact on ecosystems and guiding sustainable land management practices.

## **4.6 CONCLUSION**

This chapter outlined the data sources, tools, and methods used to assess forest fire risk zones. Various satellite, meteorological, topographic, and anthropogenic datasets were processed to generate thematic layers. Using the Analytical Hierarchy Process (AHP), these layers were weighted and integrated in a GIS environment to produce a forest fire risk map. The map was validated using NASA FIRMS hotspot data, ensuring its reliability. The combination of GIS and remote sensing tools provided a strong foundation for further analysis in the next chapter.

# **CHAPTER 5**

## **RESULT AND DISCUSSION**

### **5.1 PHYSIOGRAPHIC FACTOR**

This chapter deals with the discussion on Wildfire riskmap using Analytic Hierarchy Process (AHP) for Loa angeles , California .

#### **5.1.1 ELEVATION**

The Los Angeles elevation, a key factor in forest fire susceptibility, was analyzed using SRTM DEM data with a 30-meter spatial resolution. The elevation values were classified into five classes: 24 - 388 meters, 388 - 812 meters, 812 - 1285 meters, 1285 - 1830 meters, and 1830 - 3066 meters. Lower elevation zones are associated with higher human activity and sparse vegetation, increasing fire ignition risk. Mid-elevation ranges have dense forest cover and moderate fire susceptibility. Higher elevations have cooler temperatures, increased moisture, and unique vegetation types, reducing fire risk but potentially experiencing occasional fires due to prolonged dry spells. This classification aids in identifying areas most vulnerable to forest fires and supports effective fire management and prevention strategies

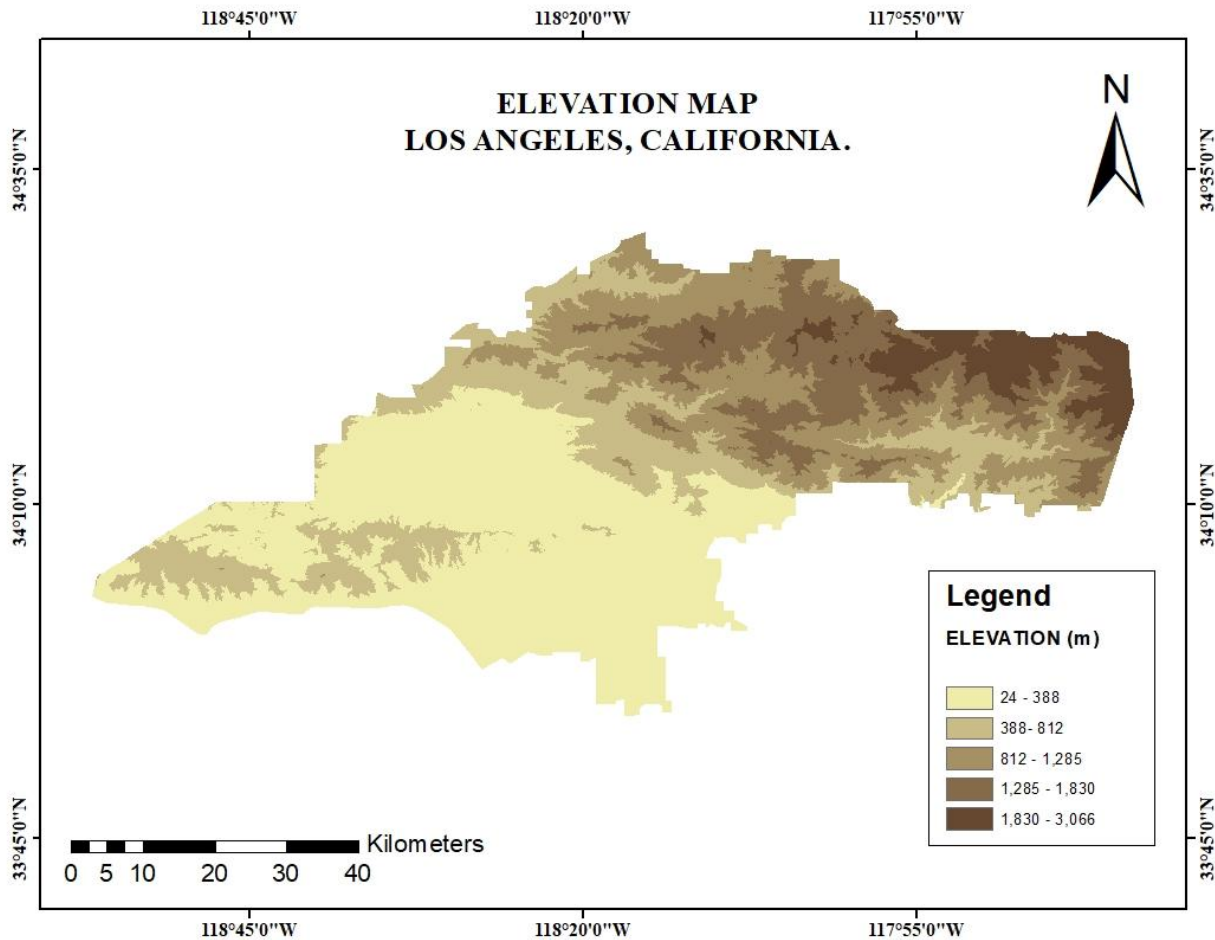


Figure-5.1 Elevation Map

### 5.1.2 SLOPE

Forest fire behavior is influenced by slopes, with fires spreading more rapidly uphill due to the upward movement of heated air and the "Chimney effect." In Los Angeles, slopes play a crucial role in determining fire susceptibility due to its complex terrain. Slopes are categorized into five classes based on the IMSD slope classification: very gentle, moderate, steep, and very steep. Gentle slopes promote vegetation growth and fuel accumulation, while moderate slopes balance fuel buildup and fire spread. Understanding these slope categories is essential for tailoring fire management strategies to the topography of Los Angeles.

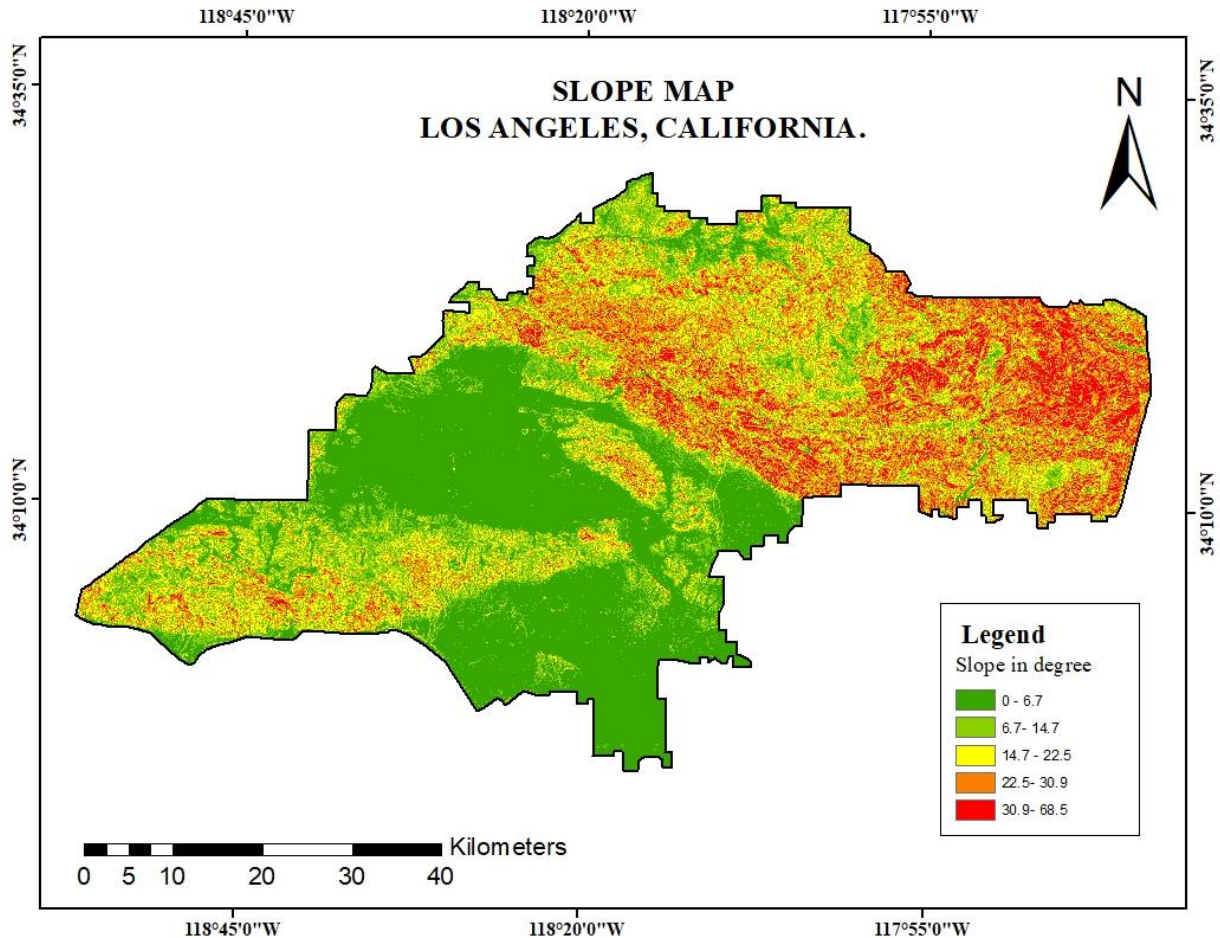


Figure-5.2 Slope Map

### 5.1.3 ASPECT

The Los Angeles terrain is classified into eight directional categories using an SRTM DEM (Digital Elevation Model) with a 30-meter spatial resolution. The terrain predominantly exhibits a South-Southeast-facing aspect, which is crucial in forest fire susceptibility studies due to factors like solar exposure, moisture retention, and wind patterns. The use of high-resolution SRTM DEM data ensures precise topographical analysis, aiding in the accurate assessment of fire-prone areas in the diverse and ecologically sensitive landscape of Los Angeles.

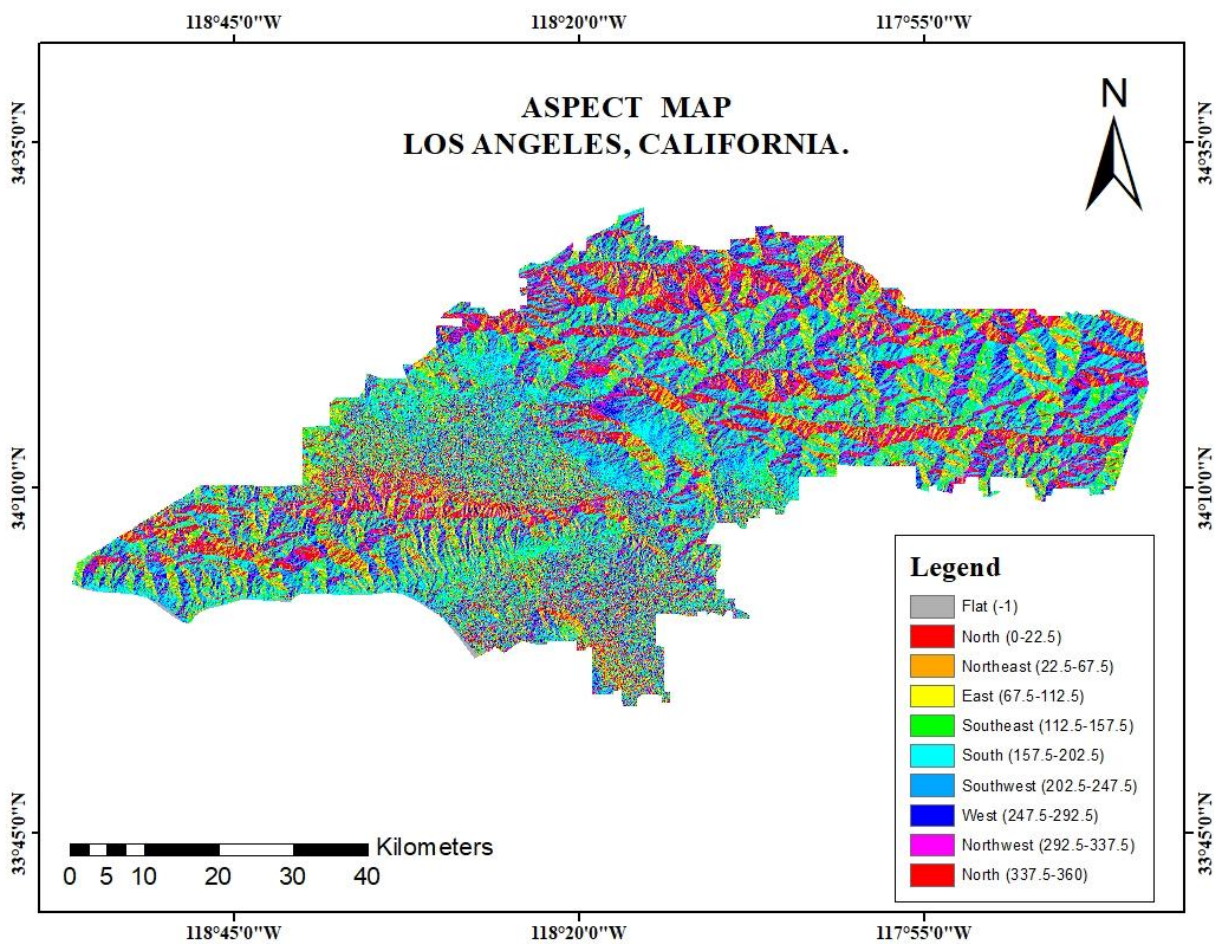


Figure-5.3 Aspect Map

#### **5.1.4 TOPOGRAPHICAL ROUGHNESS INDEX (TRI)**

The Topographic Roughness Index (TRI) is a tool used to measure the surface roughness of a landscape, estimating elevation changes within a specific neighborhood. It quantifies the extent of elevation variation among neighboring cells in a Dendrometric Model (DEM). The Los Angeles, California, USA map shows the variability in terrain ruggedness across the region. Higher TRI values indicate steep and rugged terrain, which can affect forest fire susceptibility. Rough terrain creates barriers and challenges for

firefighting, while smoother areas facilitate rapid fire spread. Understanding TRI distribution helps identify high-risk zones and plan effective fire management strategies.

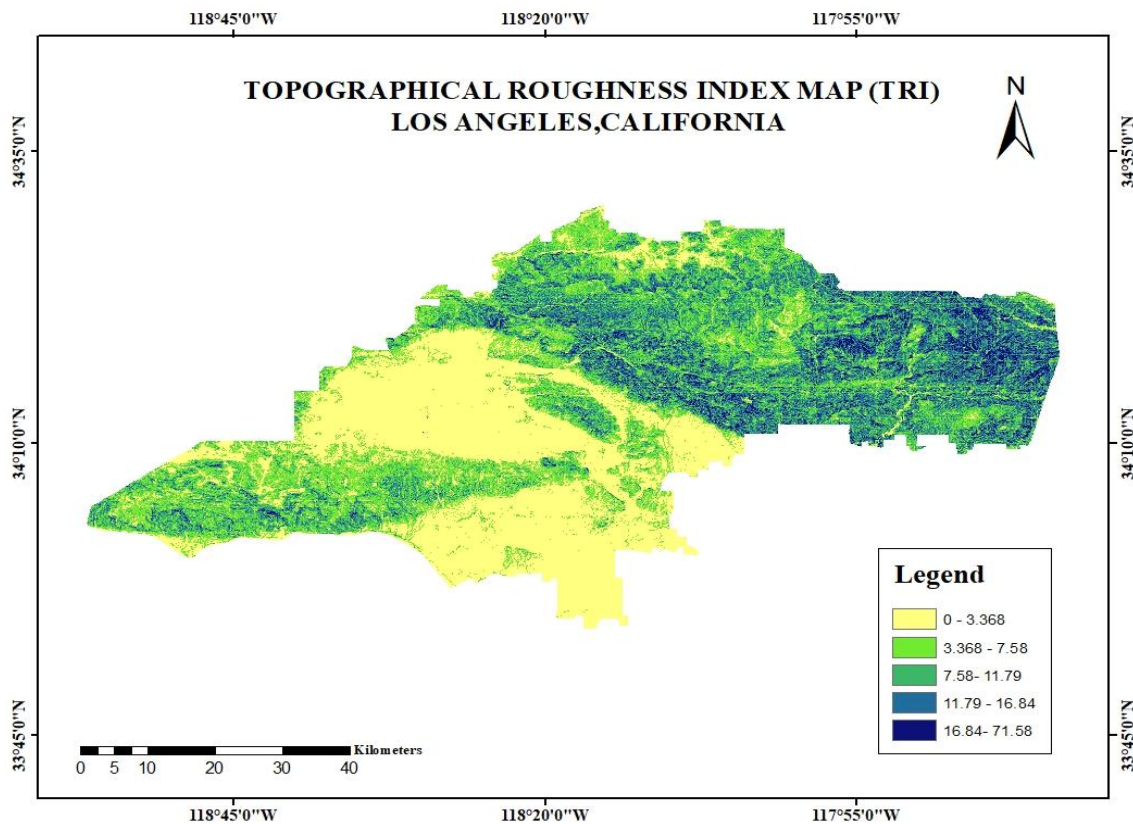


Figure-5.4 TRI Map

### **5.1.5 LANDUSE AND LANDCOVER**

Changes in LULC significantly affect the occurrence of forest fire. An increase or decrease in the abundance of vegetation and changes in its composition can result in increases or decreases in forest fires. The Landuse/Landcover (LULC) map of the Los Angeles, California, USA, reveals a diverse landscape comprising vegetation, trees, crops, bare grounds, build-up areas, range lands, snow/ice, and water bodies. Each land cover type contributes uniquely to forest fire susceptibility in the region. Trees are high-risk areas for forest fire due to abundance of dry vegetation that can act as fuel. Vegetation, often

with uniform tree species, may also be prone to rapid fire spread. On the other hand, crops and range lands can contribute to localized fire risks, especially during harvest seasons or periods of dry weather. Bare ground and built-up areas are generally less susceptible to forest fires but may act as firebreaks, preventing the spread of fires. Water bodies and their surrounding areas provide natural fire barriers and help reduce susceptibility. This LULC information is crucial for identifying vulnerable zones and implementing targeted fire prevention and management strategies in the Los Angeles

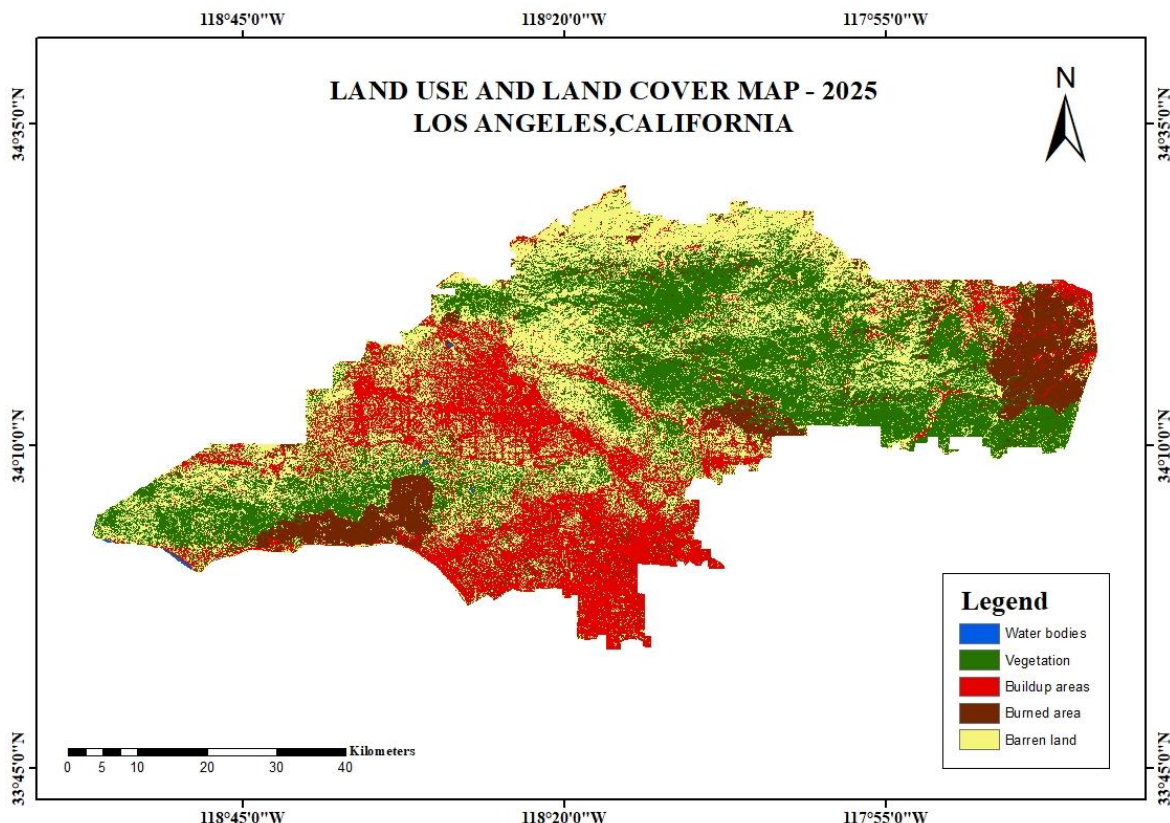


Figure-5.5 LULC Map

### 5.1.6 NORMALIZED BURN RATIO (NBI)

NBR stands for Normalized Burn Ratio. It's a spectral index used primarily to identify and assess burned areas and the severity of wildfires using remote sensing data, especially from satellites like Landsat.

$$\text{NBR} = (\text{NIR} - \text{SWIR}) / (\text{NIR} + \text{SWIR})$$

NIR (e.g., Band 5 in Landsat 8): Reflects healthy vegetation. SWIR (e.g., Band 7 in Landsat 8): Sensitive to moisture content; higher in burned or dry areas. Values range from -1 to +1, with lower values (especially negative) indicating burned or damaged vegetation, while higher values represent healthy, unburned vegetation. On the January 6 map, significant fire-affected areas are visible in red (NBR values between -0.99 and -0.58), particularly in the northeastern and southwestern regions of Los Angeles. Yellow areas indicate moderate impact, while the widespread green areas (NBR 0.18 to 0.99) reflect healthy vegetation. In comparison, the January 14 map shows an expansion of burned regions, especially in the southwestern and southeastern parts, indicating ongoing or newly detected fire damage. Some areas previously shown as unaffected or moderately affected have transitioned to lower NBR values, suggesting worsening conditions. Overall, the maps reveal a notable progression of fire impact over the eight-day period.

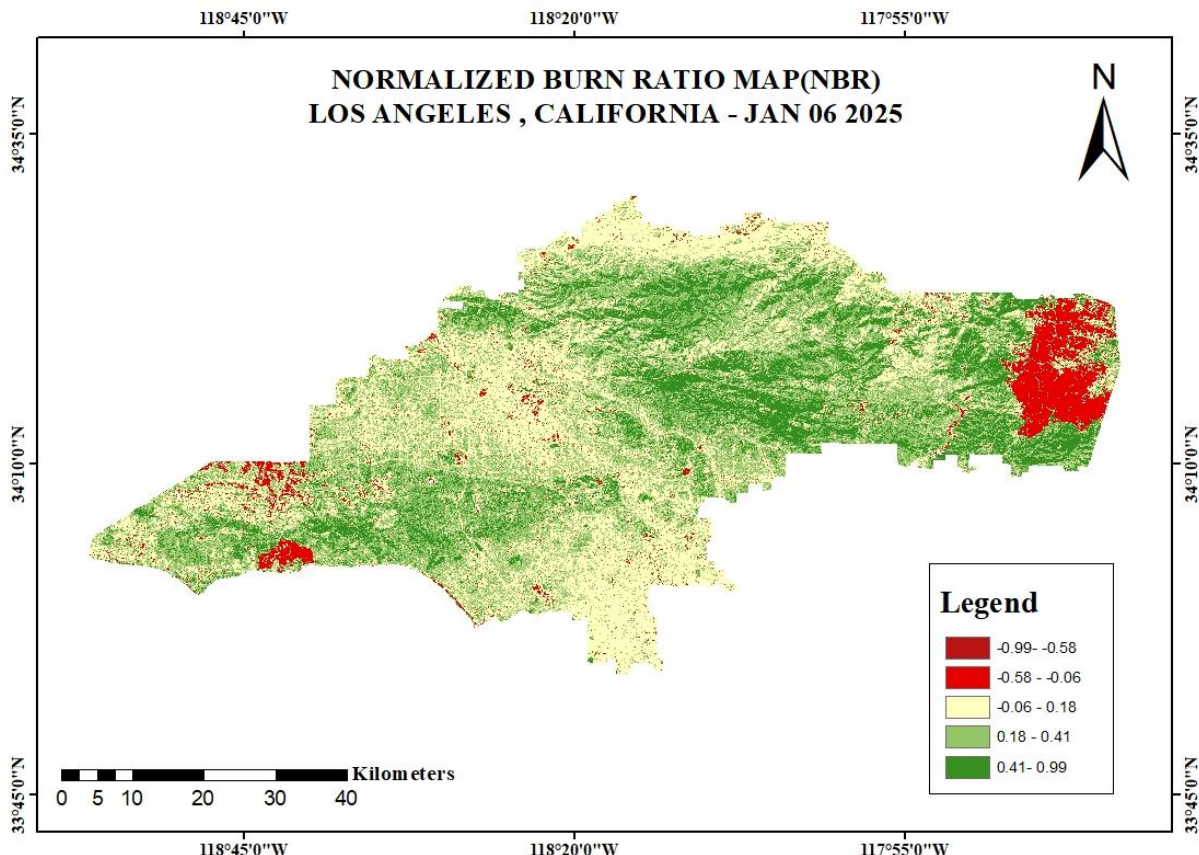


Figure-5.6 NBR (06/01/2025)

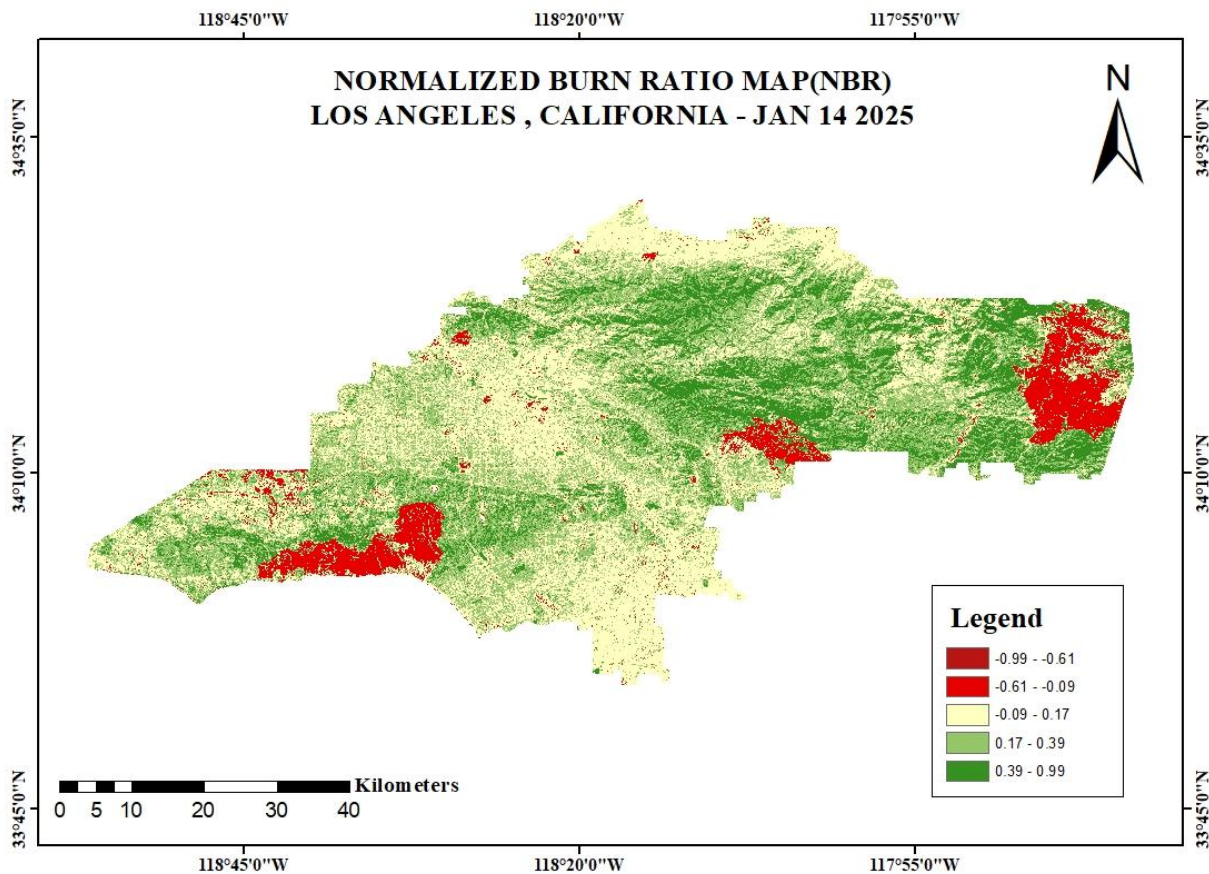


Figure-5.7 NBR (14/01/2025)

### **5.1.7 DIFFERENTIAL NORMALIZED BURN RATIO (dNBR)**

dNBR is a commonly used index to assess the severity of wildfires by comparing the Normalized Burn Ratio (NBR) before and after a fire. It highlights the differences in the landscape caused by the fire, helping to evaluate the extent and severity of the burn.

Formula:

$$dNBR = (NBR_{\text{prefire}}) - (NBR_{\text{postfire}})$$

Where:

NBR<sub>pre-fire</sub> is the Normalized Burn Ratio calculated from satellite data before the fire.

NBR\_post-fire is the Normalized Burn Ratio calculated from satellite data after the fire.

The map uses a color-coded scale to indicate significant vegetation loss, with red shades indicating significant areas, yellow areas indicating minimal to no change, and green areas indicating areas where vegetation might have improved due to seasonal changes, regrowth, or data variation. The most severely affected zones are concentrated in distinct clusters, aligning with active fire zones. The widespread yellow indicates stability, while localized severe impacts are clearly delineated, aiding in prioritizing post-fire recovery and management efforts. This spatial pattern confirms the progression and impact of wildfires over the observed time frame.

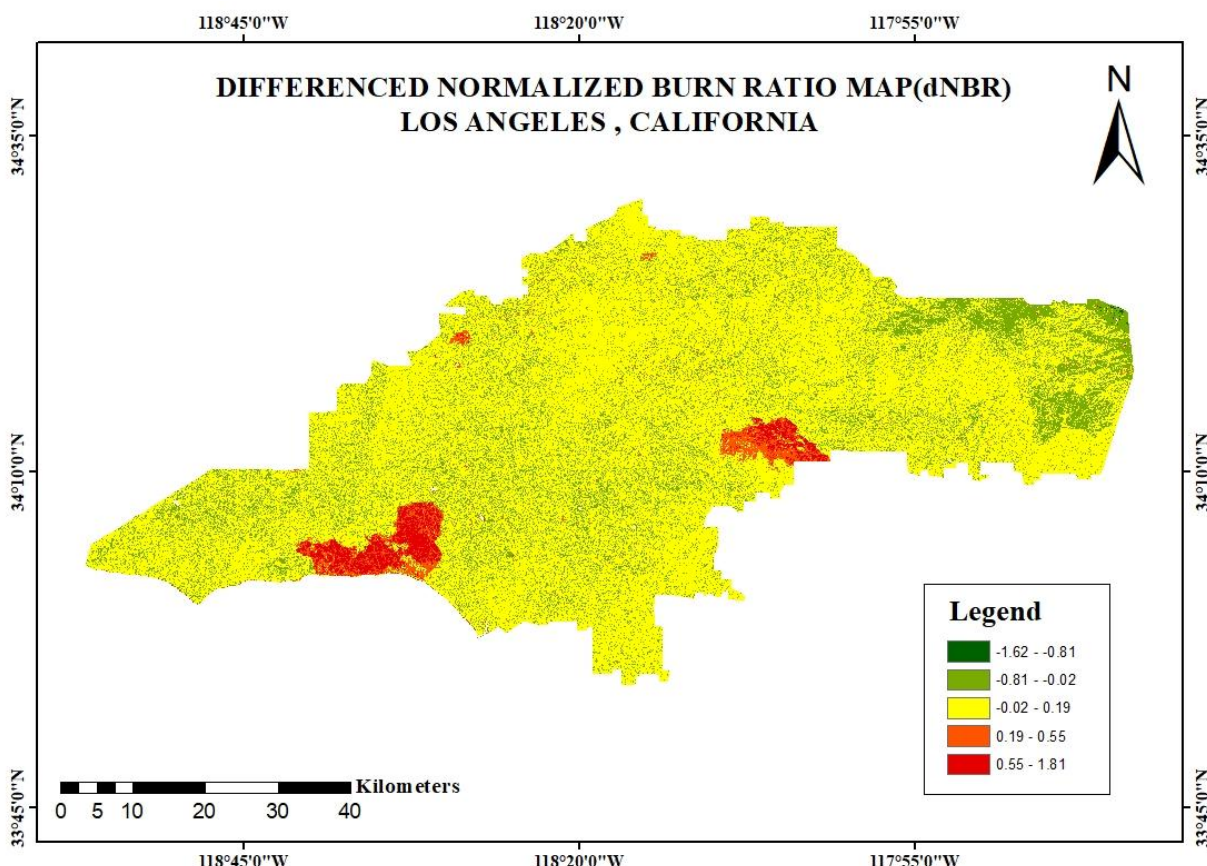


Figure-5.8 dNBR

## **5.1.8 NORMALIZED DIFFERENCE VEGETATION INDEX (NDVI)**

The Normalized Difference Vegetation Index (NDVI) is a widely used remote sensing index that measures vegetation health and density based on the reflectance of near-infrared (NIR) and red light. In this study, NDVI values were extracted from Landsat 9 OLI/TIRS imagery with a spatial resolution of 30 meters, presenting detailed vegetation analysis for the Los Angeles. The NDVI values were classified into five categories to evaluate forest fire susceptibility. These classes include: very low , low , moderate , high , and very high . NDVI data can be used to determine the intensity of a forest fire after it has occurred. Post-fire areas with statistically lower NDVI values demonstrate extensive vegetation degradation. This type of data is crucial for post-fire recovery and restoration operations. This classification helps to identify areas with varying levels of vegetation density, where lower NDVI values often correspond to sparse or stressed vegetation, potentially indicating higher susceptibility to forest fires. By integrating NDVI with elevation data, this analysis provides valuable insights for forest management and fire risk mitigation in the ecologically sensitive Los Angeles region

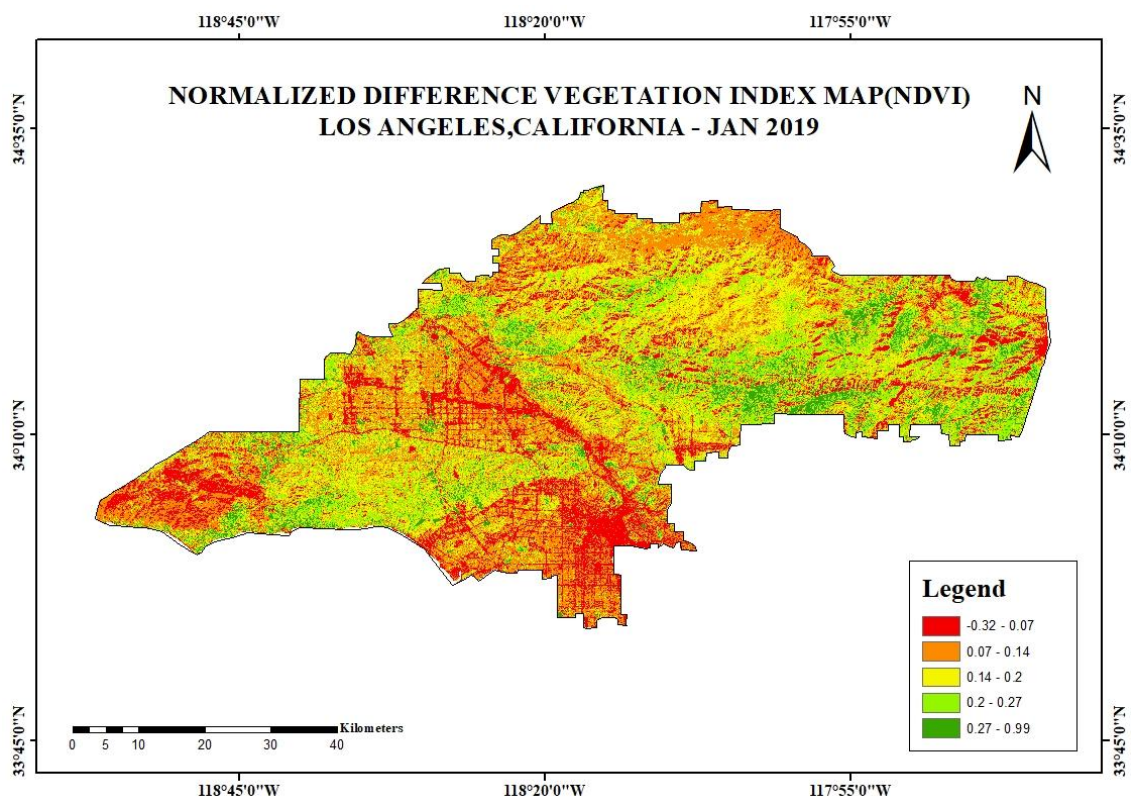


Figure-5.9 NDVI-2019

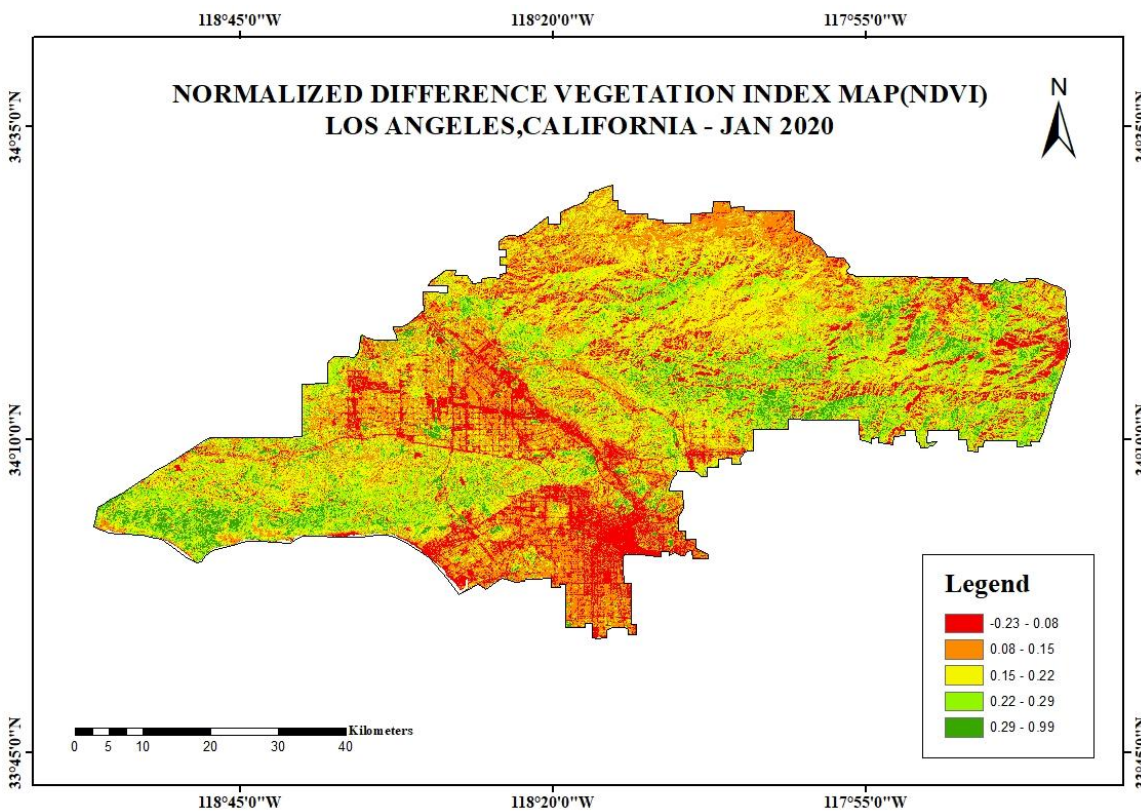


Figure-5.10 NDVI- 2020

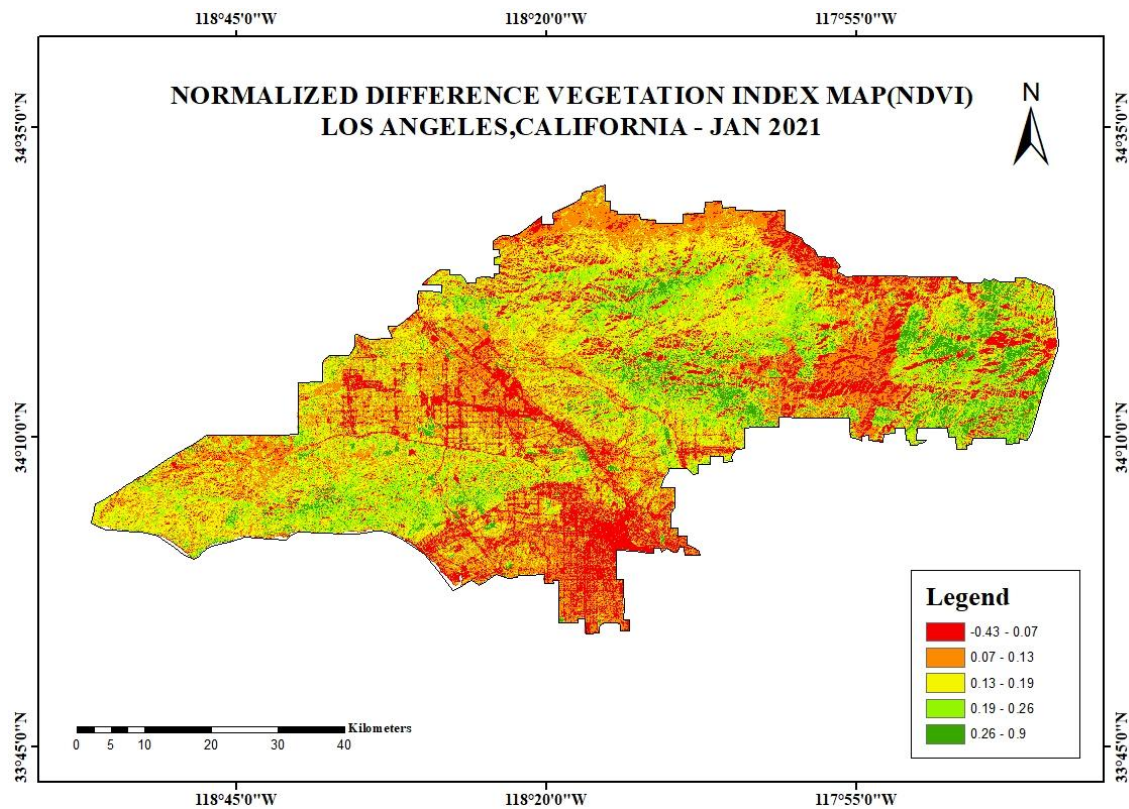


Figure-5.11 NDVI-2021

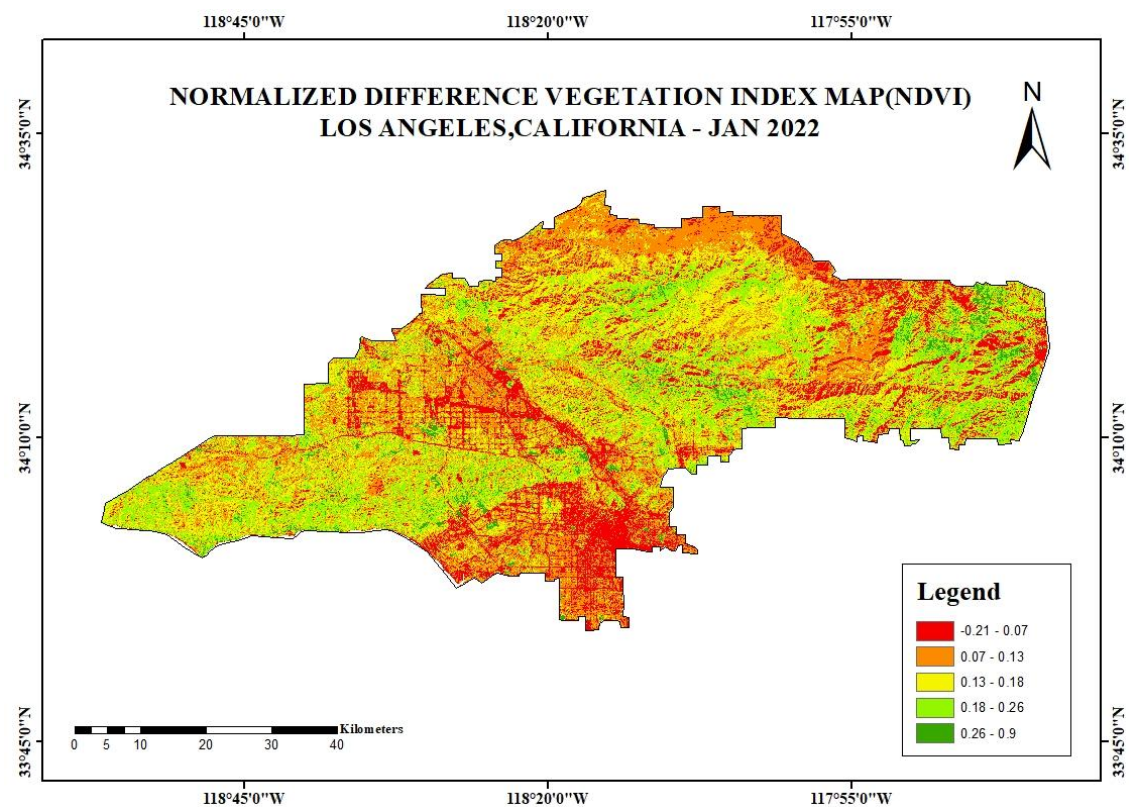


Figure-5.12 NDVI-2022

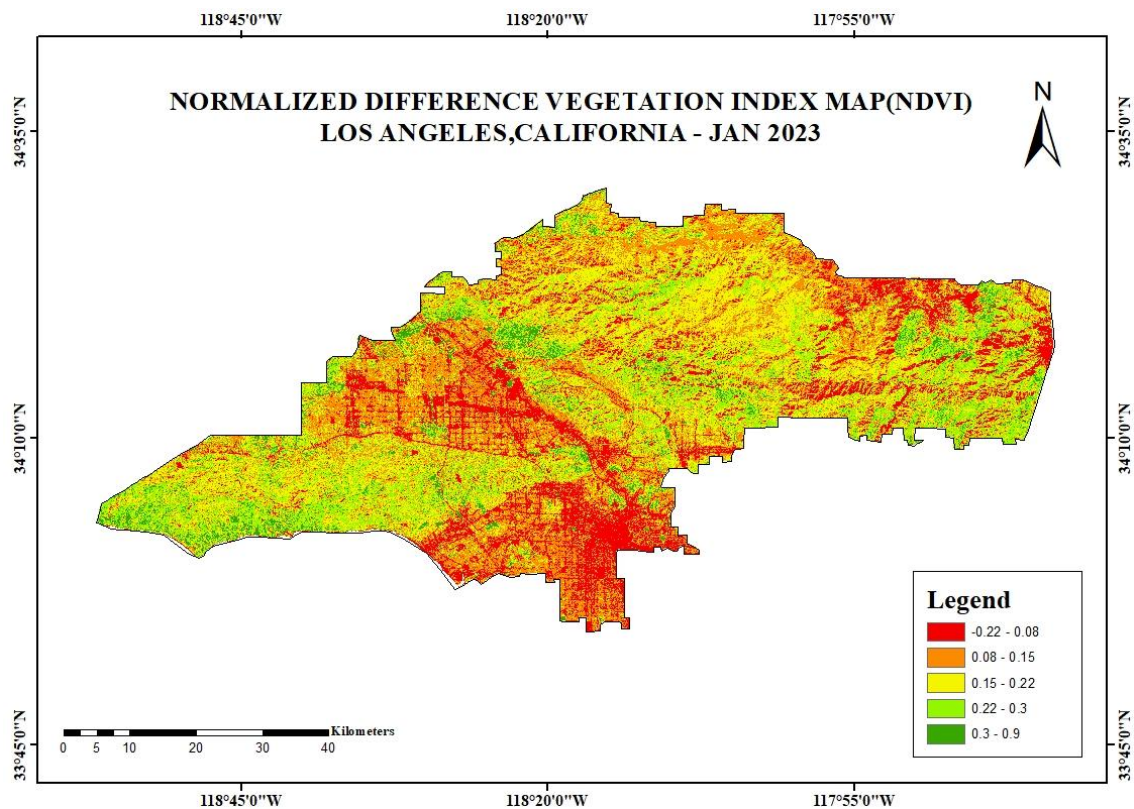


Figure-5.13 NDVI-2023

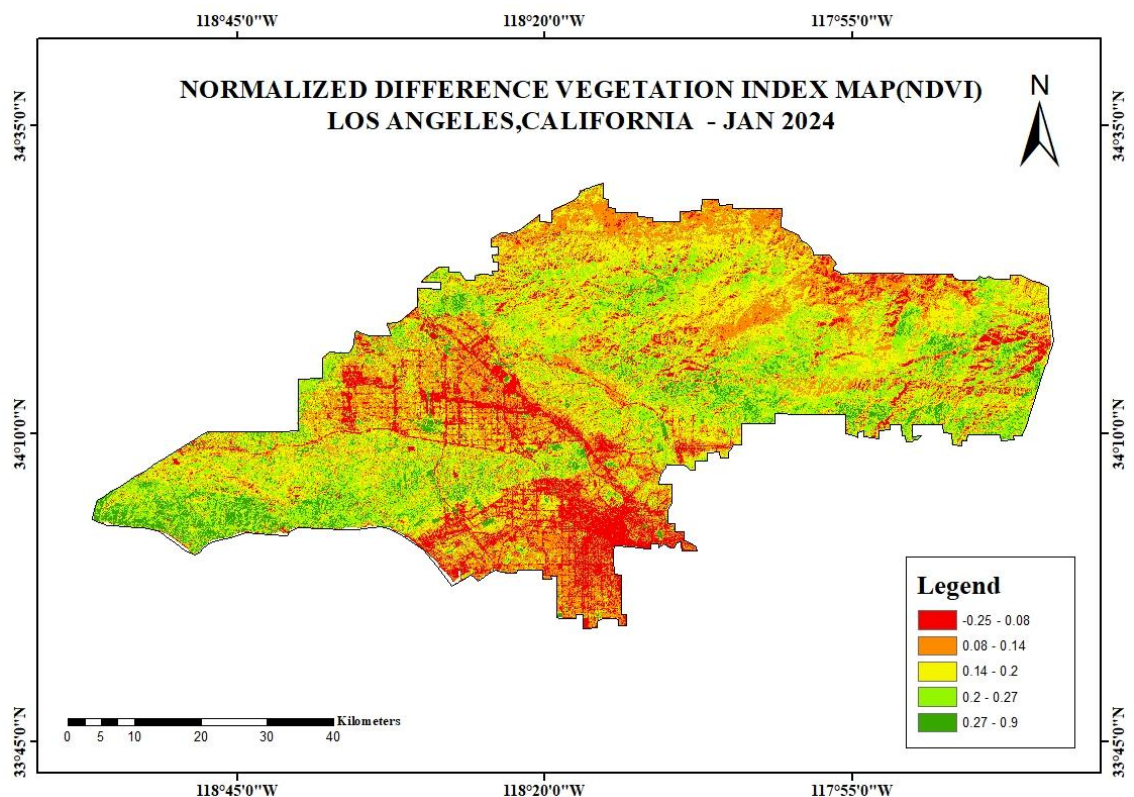


Figure-5.14 NDVI-2024

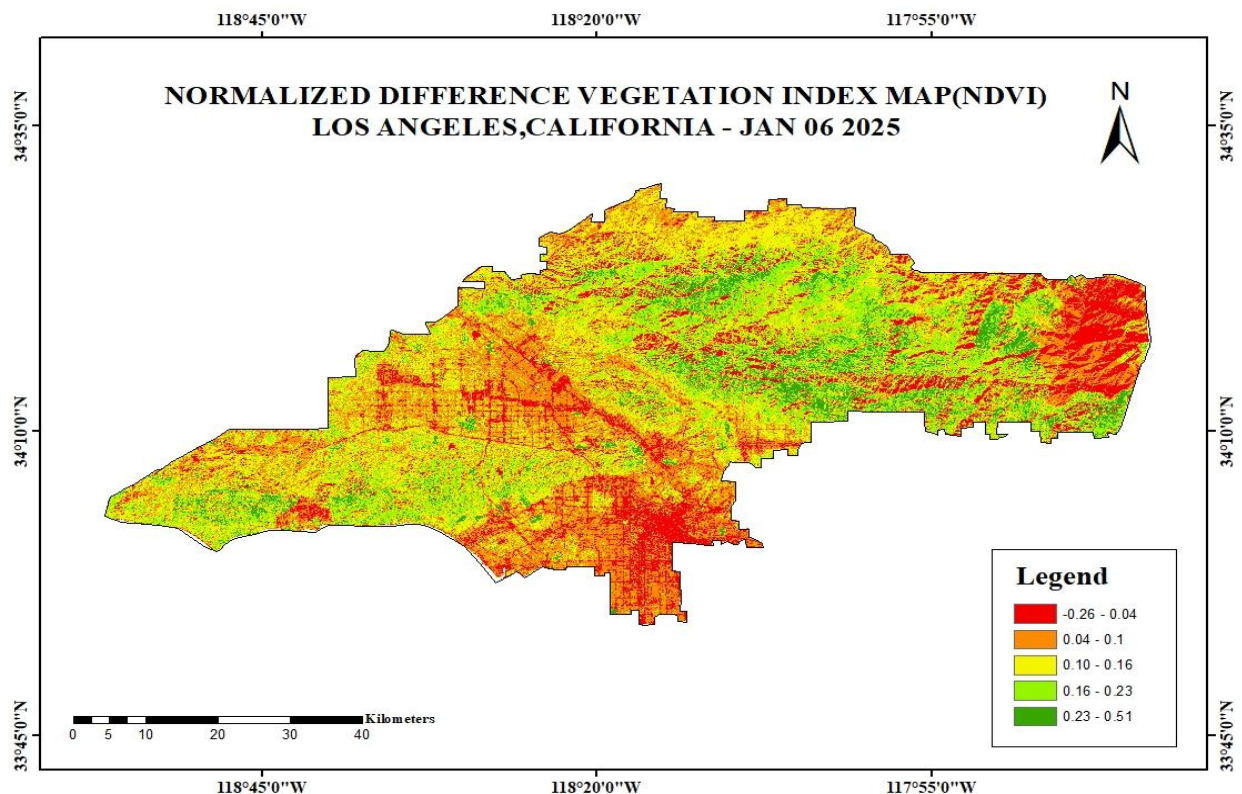
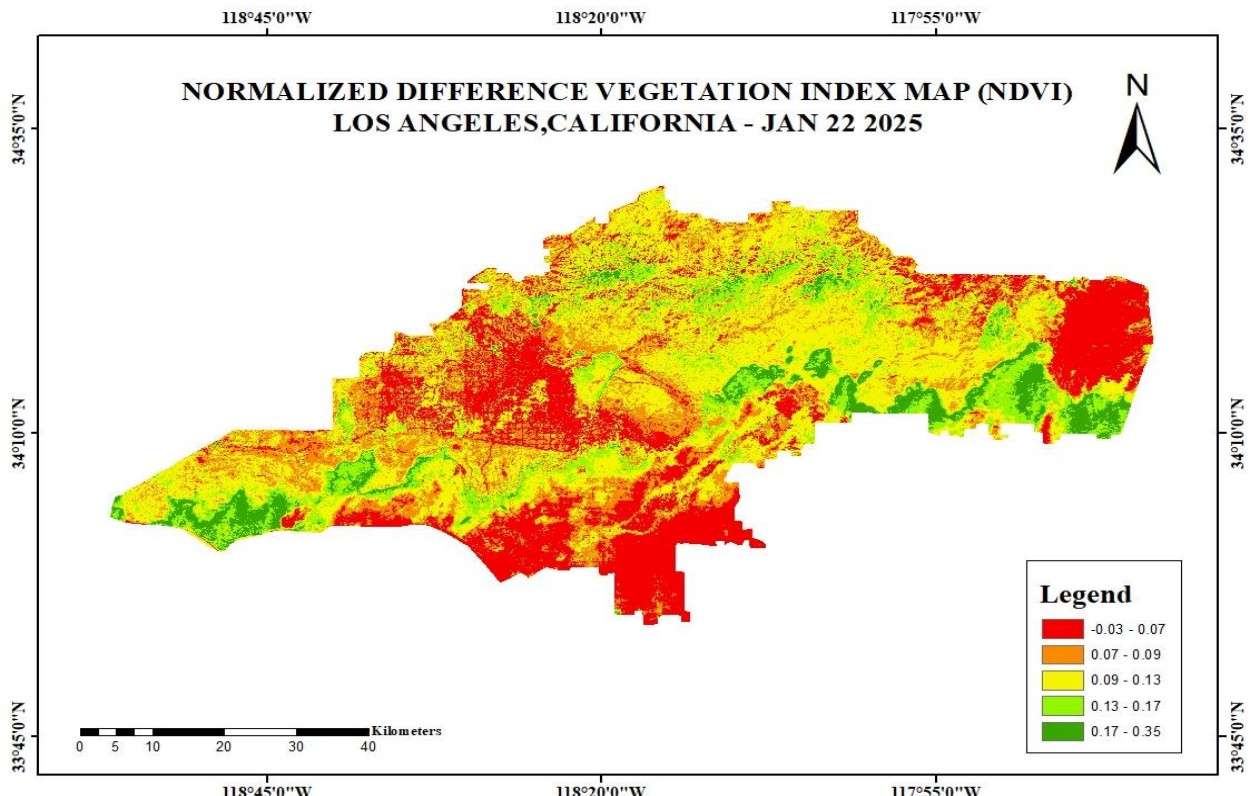


Figure 5.15 Before Forestfire in losAngeles (06/01/2025)



After Forestfire in losAngeles (22/01/2025)

## **5.2 DAMAGE ASSESSMENT**

The Damage Assessment map gives a clear visual impression of the spatial pattern and severity of damage in the area. It classifies the degree of damage into five different levels: very low (dark green), low (light green), moderate (yellow), high (orange), and very high (red). These are color-coded to indicate the different intensities of destruction throughout the landscape. The most impacted zones, highlighted in orange and red, are largely in the southwestern and central regions of the map. Besides, black dots also signify burnt buildings, which are concentrated in the same high and very high damage areas. This pattern of distribution points to the relationship between structural loss and areas of severe damage as indicating localized episodes of severe impact, like wild fire or other large-scale catastrophe

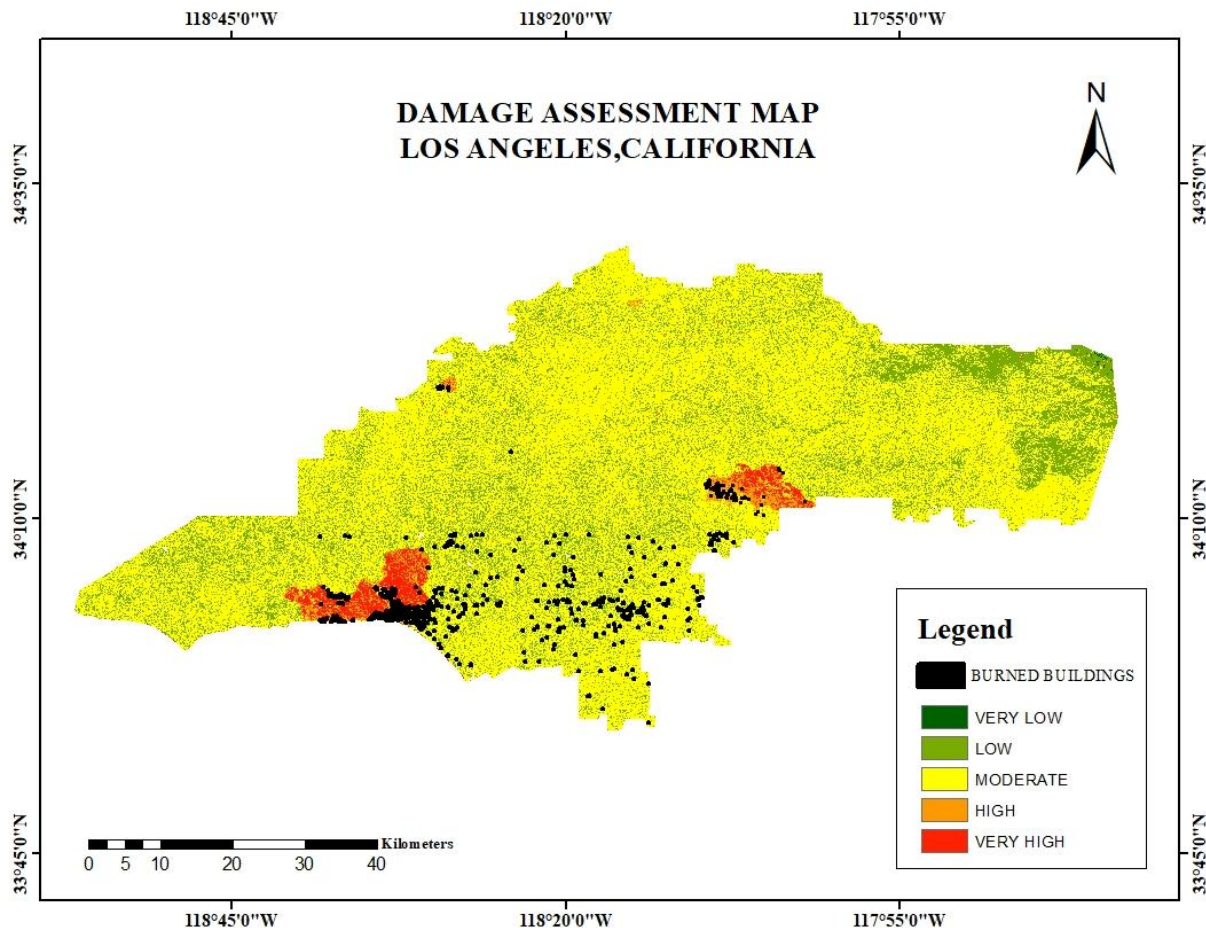


Figure 5.16 Damage Assessment

## **5.3 CLIMATIC FACTOR**

### **5.3.1 LAND SURFACE TEMPERATURE**

Land Surface Temperature (LST) is the radiative skin temperature of the land derived from solar radiation. LST, the skin temperature of the ground, is identified as a significant variable of microclimate and radiation transfer within the atmosphere. For the current study, Landsat 9 with the Thermal bands can facilitate LST calculation by the formula:

$$LST = BT / I + W * (BT / p) * \ln(e)$$

Where,

LST - Land Surface Temperature,

e - Emissivity,

BT - Brightness Temperature,

p – 14380, W-Wavelength of emitted radiance (11.5 $\mu$ m).

The steps involved in calculating the Land surface temperature are:

STEP 1: Calculation of TOA (Top of Atmospheric) spectral radiance.

$$TOA(L) = ML * Qcal + AL$$

STEP 2: TOA to Brightness Temperature conversion

$$BT = (K2 / (\ln(K1 / L) + 1)) - 273.15$$

STEP 3: Calculation of NDVI

$$NDVI = (Band 5 - Band 4) / (Band 5 + Band 4)$$

STEP 4: Calculate the proportion of Vegetation (P<sub>v</sub>)

$$P_v = \text{Square} ((\text{NDVI}-\text{NDVImin}) / (\text{NDVImax}-\text{NDVImin}))$$

STEP 5: Calculate Emissivity  $\epsilon$

$$\epsilon = 0.004 * P_v + 0.986$$

STEP 6: Calculate the Land Surface Temperature

$$LST = BT/I + W * (BT/p) * \ln(e)$$

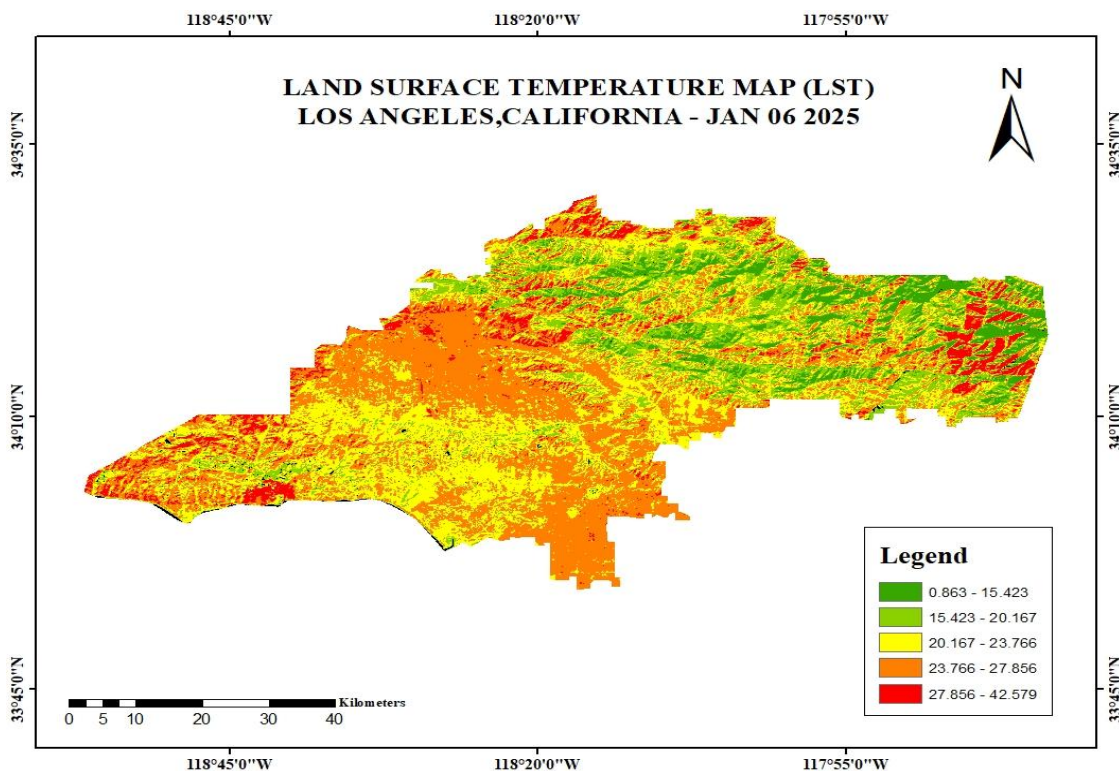
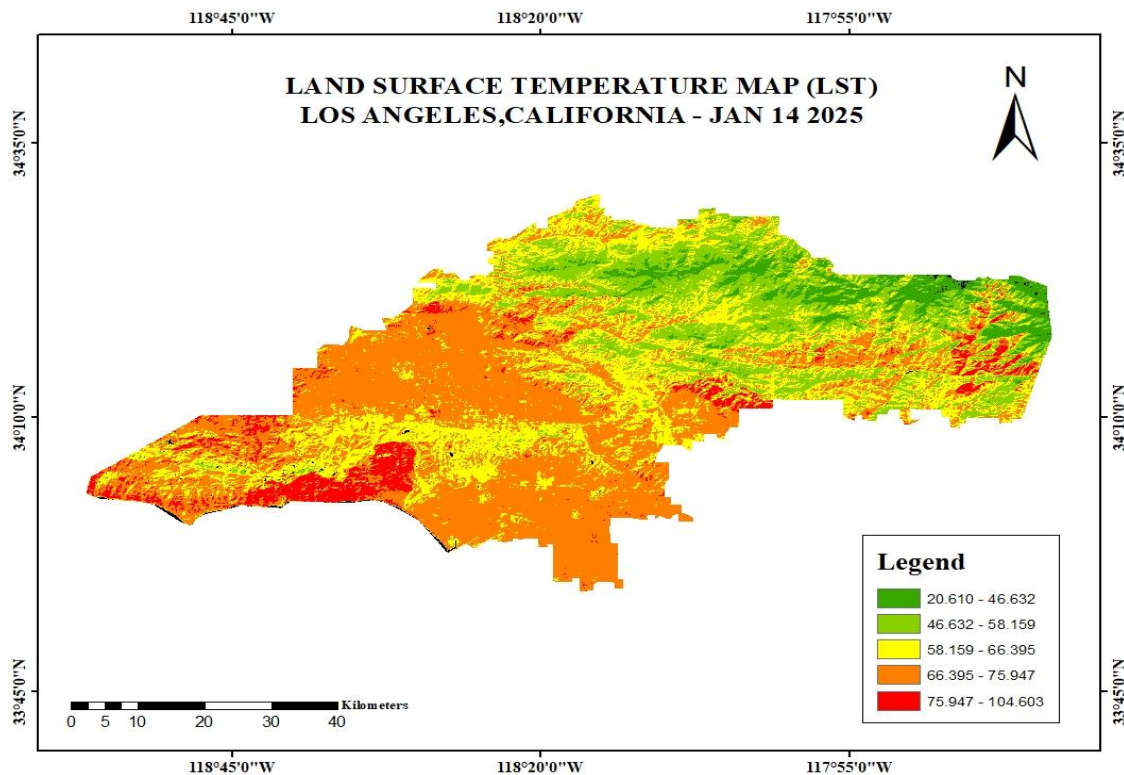


Figure 5.17  
Before Forestfire in losAngeles (06/01/2025)



After Forestfire in losAngeles (22/01/2025)

### **5.3.2 WIND DIRECTION**

The above map illustrates the spatial distribution of average wind direction across Los Angeles County for the period from January 1st to January 30th. The area is divided into zones represented by different colour gradients, each indicating a specific wind direction range in degrees. These directional values, ranging from  $5.99^\circ$  to  $271.89^\circ$ , are categorized into five distinct classes as shown in the legend. Northeastern and central regions experience predominant wind directions between  $5.99^\circ$  and  $89.41^\circ$ , as indicated by the brown and tan zones. Conversely, the southwestern parts are influenced by wind directions ranging from  $130.07^\circ$  to  $271.89^\circ$ , reflected by the green to blue shades. The central portion shows a transitional wind flow pattern, possibly influenced by topographic variation and urban land use. The use of a directional gradient aids in identifying dominant wind patterns, which are critical for air quality analysis, wildfire behaviour modelling, and urban planning. The classification scheme effectively captures spatial

variability in wind patterns, contributing valuable insight into atmospheric dynamics during the winter season in Southern California.

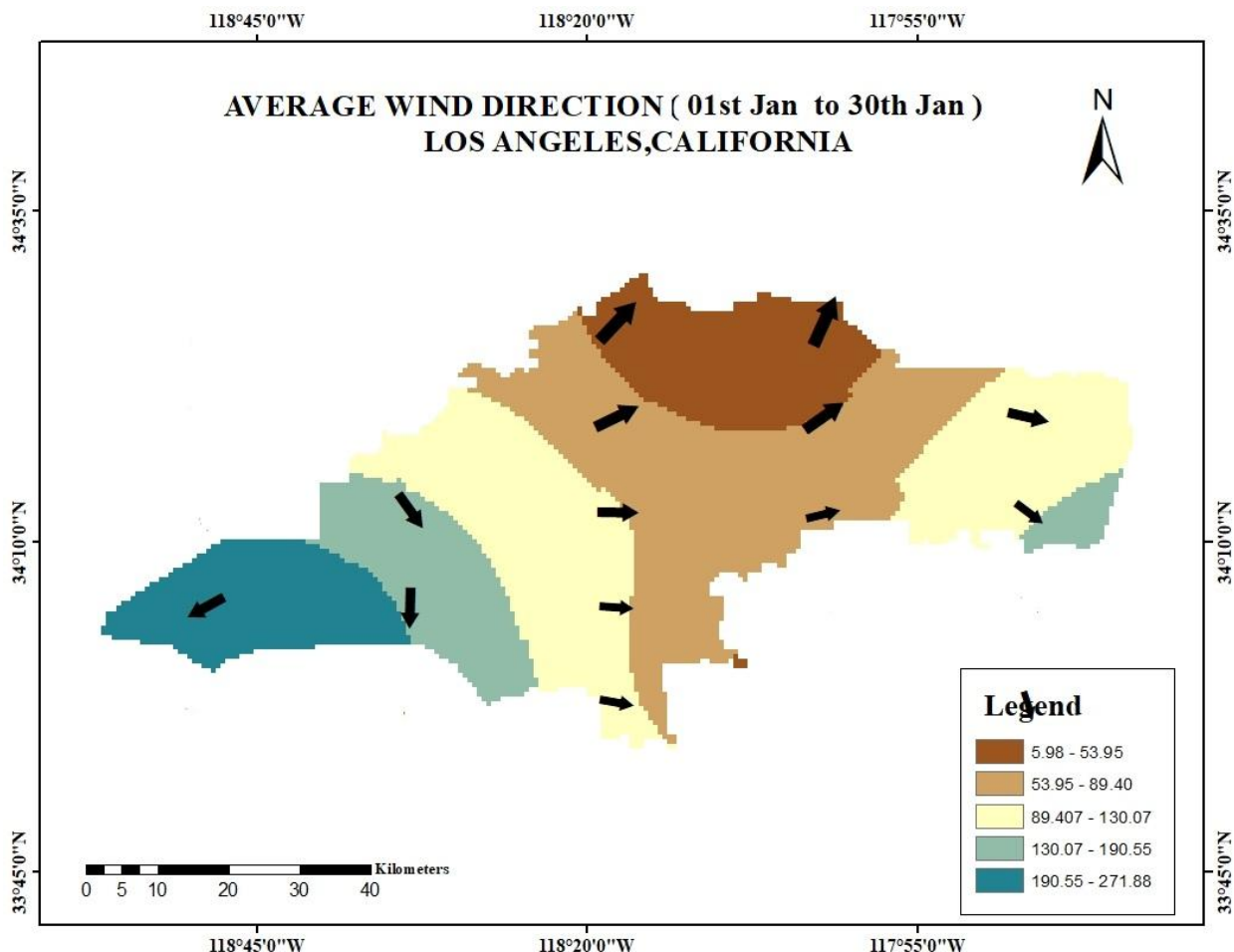


Figure 5.18 Wind direction

### 5.3.3 WIND SPEED

The above map visualizes the spatial distribution of average wind speed across Los Angeles County for January 2025. The region is divided into zones represented by a five-class color gradient, illustrating wind speeds ranging from 14.51 km/h to 45.96 km/h. The lightest shades in the southeastern part of the county indicate lower wind speeds between 14.51 and 24.63 km/h. In contrast, the darkest tones, found in the western and northwestern areas, reflect significantly higher wind activity ranging from 38.68 to 45.96

km/h. This west-to-east gradient in wind intensity may be influenced by topographical features, coastal effects, and seasonal atmospheric patterns, including Santa Ana winds. The central regions display a gradual transition in wind speed, supporting the presence of localized microclimatic variations. This spatial analysis of wind speed is essential for modeling wildfire behavior, assessing air quality impacts, and informing urban planning strategies during Southern California's winter months.

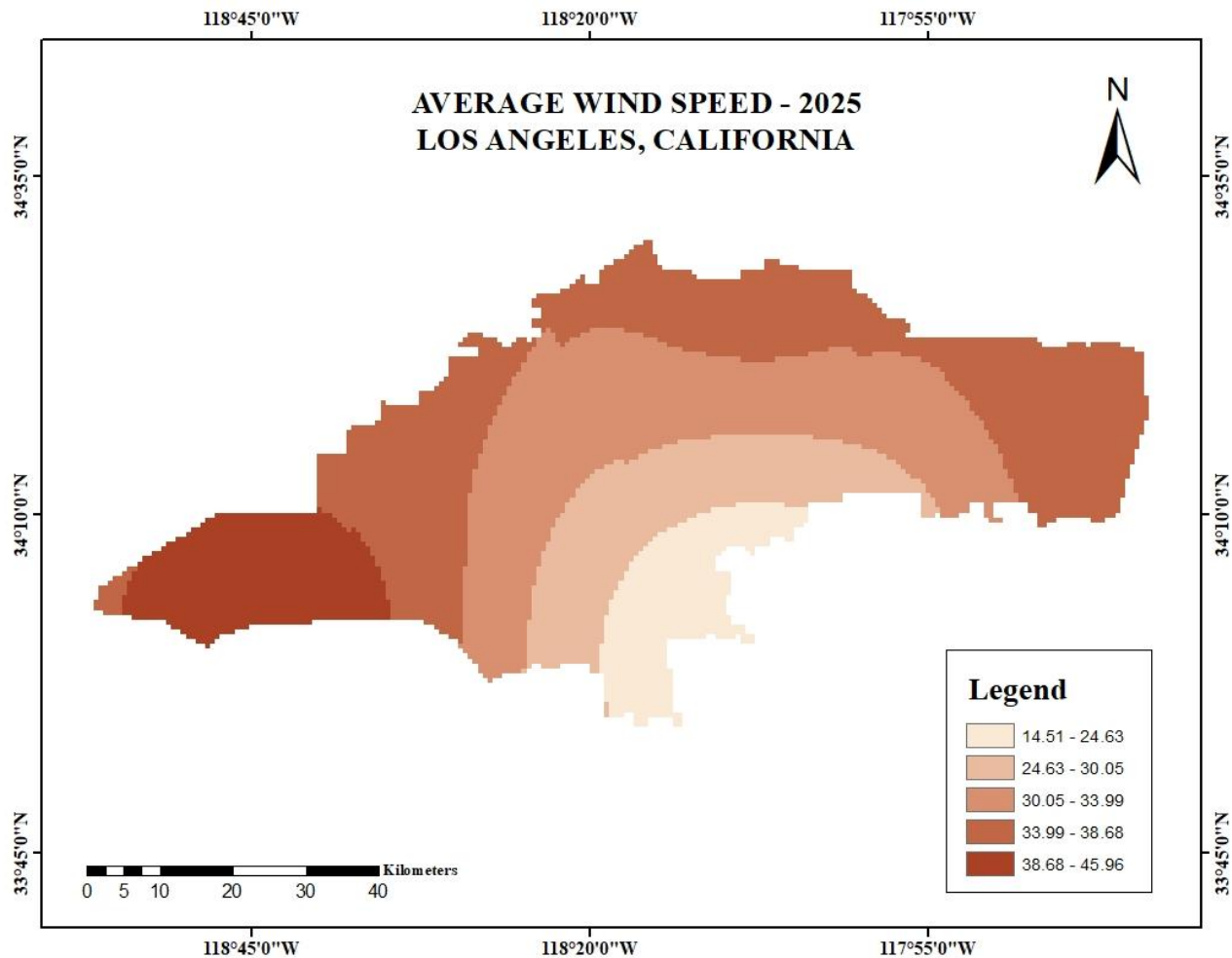


Figure 5.19 Wind Speed

## **5.4 ANTHROPOGENIC FACTOR**

### **5.4.1 PROXIMITY OF ROAD**

This map in Los Angeles, California, shows the proximity of different areas to major roads. The map is color-coded based on the distance from the roads, with brown areas representing areas directly on the roads (0 meters away). As the distance from the roads increases, the colors change, creating buffer zones around the road network. The scale bar at the bottom provides a distance reference and a north arrow for orientation. Latitude and longitude coordinates are shown around the map's borders using degrees, with negative longitudes indicating locations west of the Prime Meridian. The map effectively highlights the spatial variation of road access across the city, with densely road-proximal areas in the central and southern parts and more distant zones in the outskirts.

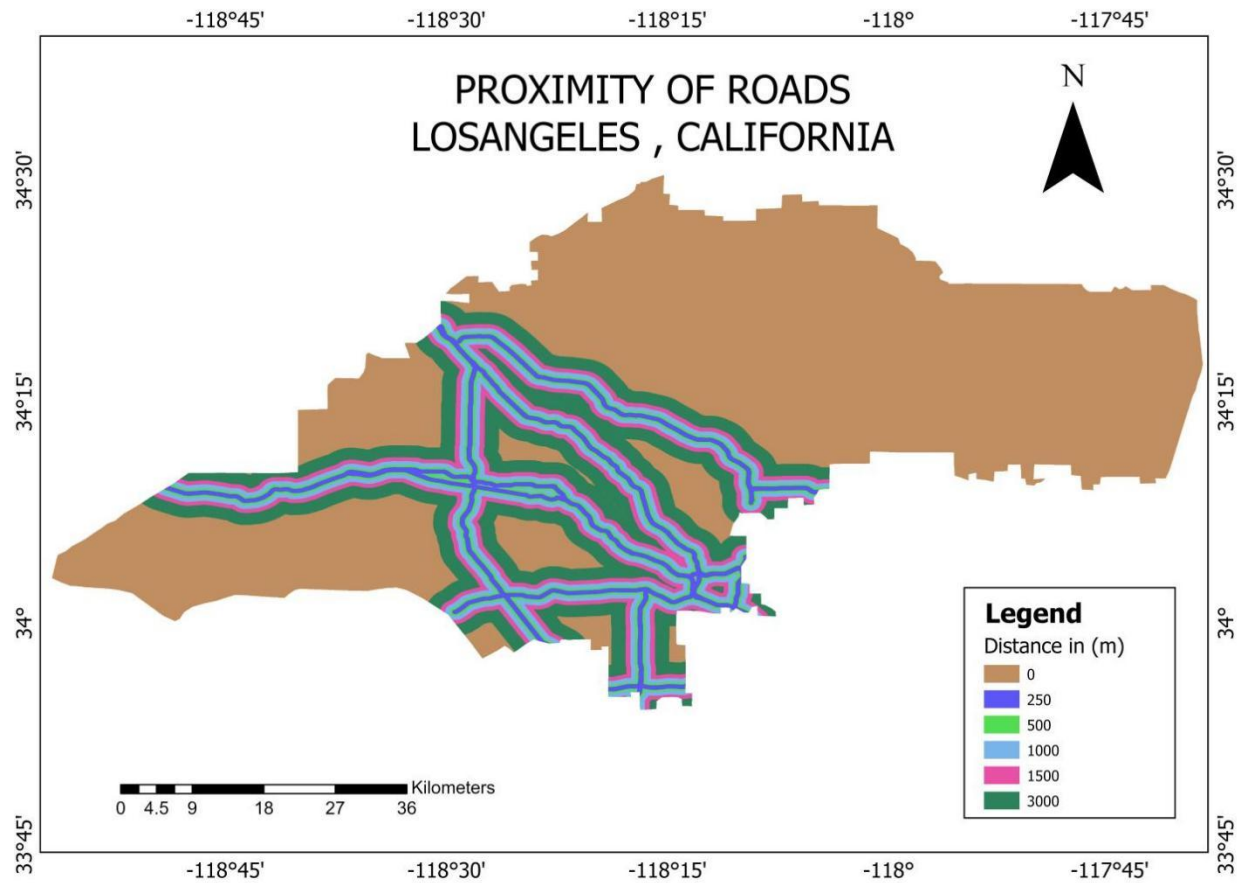


Figure 5.20 Proximity of Road

#### **5.4.2 PROXIMITY OF SETTLEMENTS**

The map titled "Proximity of Settlements – Los Angeles, California" displays the spatial distribution of buildings in relation to distance zones within Los Angeles County. This type of analysis is crucial for disaster risk assessment, as it helps identify which buildings are most vulnerable and may require immediate attention or evacuation. It supports emergency response planning by guiding where to position resources like shelters, fire stations, or medical aid. The central polygon represents the county boundary used as the study area. Five concentric distance bands, each represented by a distinct color, illustrate how far settlements (buildings) are located from the edge of the study area. These zones are categorized by distance in kilometers: the green zone represents areas within 1 kilometer from the boundary, followed by purple, red, blue and

orange. The legend in the lower right corner provides a clear reference to these distance classes. A north arrow and a scale bar are included to provide orientation and a sense of distance, while geographic coordinates (latitude and longitude) frame the map for spatial reference. This map can be used to assess settlement patterns and their proximity to the edge of the region, which is useful for disaster preparedness, land-use planning, and risk assessment related to environmental hazards such as wildfires

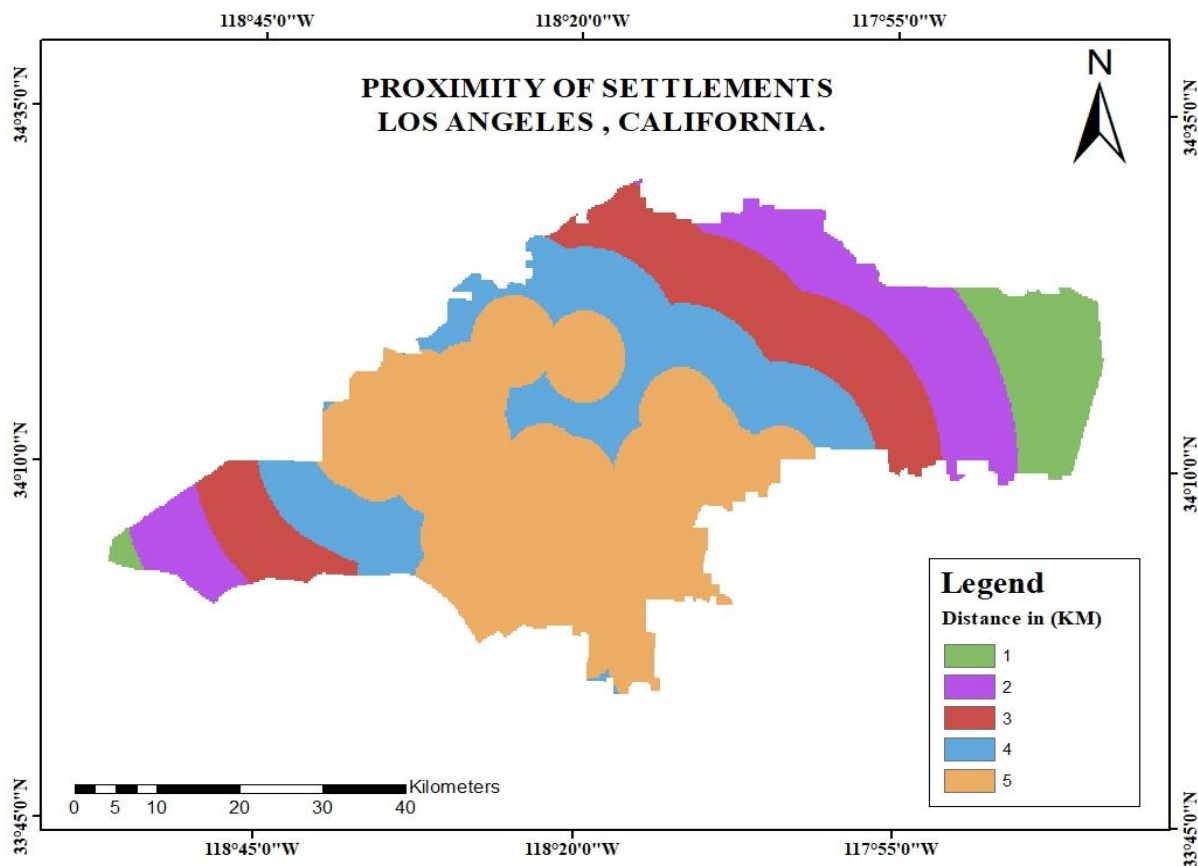


Figure 5.21 Proximity of Settlements

## **5.5 ANALYTIC HIERARCHY PROCESS (AHP) METHOD:**

The Analytical Hierarchy Process (AHP) is a structured decision-making methodology developed by Thomas L. Saaty in the 1970s, designed to solve complex

decision problems involving multiple criteria and alternatives. AHP breaks down a problem into a hierarchical structure, where the goal is at the top, followed by criteria and sub-criteria, and alternatives at the bottom. The process involves pairwise comparisons, where elements are compared in terms of their relative importance, generating a matrix of comparisons. From this matrix, the weights of criteria are derived, reflecting their relative importance. These weights are then used to rank and evaluate alternatives. AHP also includes a consistency check to ensure the reliability of the decision-making process. Widely used in fields such as environmental management, land use planning, and flood vulnerability assessment, AHP helps incorporate both qualitative judgments and quantitative data. For instance, it has been applied in GIS-based analyses for flood-prone area delineation, supporting informed decision-making for resource allocation and risk management (Saaty, 1980; Saaty, 2008; Chien et al., 2002)

### **5.5.1 PAIR WISE COMPARISON MATRIX**

In the Analytical Hierarchy Process (AHP), the Pair-Wise Comparison Matrix is used to determine the relative importance of various criteria or alternatives by comparing them in pairs. Each pair of elements is assigned numerical value on a scale typically ranging from 1 to 9, where 1 indicates equal importance and values like 3, 5, 7, and 9 represent varying degrees of preference (Saaty, 1980). The comparisons are reciprocal, meaning that if Criterion A is more important than Criterion B with a score of 3, the matrix will reflect a score of 1/3 for the comparison of B to A (Saaty, 2008). Once the comparisons are made, scale weights are calculated by normalizing the matrix and determining the principal eigenvector, which provides the proportional importance of each criterion or alternative (Chien et al., 2002). These weights are then used to rank and evaluate alternatives, converting subjective judgments into quantifiable values for decision-making. The Pair-Wise Comparison Matrix is a crucial tool in AHP, enabling a systematic and consistent approach to decision-making by organizing expert opinions and generating reliable, quantifiable outcomes

<b>Intensity</b>	<b>Description</b>	<b>Explanation</b>
1	Equal importance	Two elements contribute equally to the objective.
2	Weak/ slight	Slight preference of one over the other.
3	Moderate importance	Experience slightly favors one over the other.
4	Moderate plus	Between moderate and strong importance.
5	Strong importance	Strongly favors one over the other.
6	Strong plus	Between strong and very strong.
6	Strong plus	Between strong and very strong.

**Table -3**

Factors	NDVI	LST	WS	PR	PS	LULC	dNBR	ELEVATION	SLOPE	ASPECT	TRI
NDVI	1	4	3	2	3	3	5	2	2	2	2
LST	1/4	1	4	3	2	3	4	2	2	2	2
WS	1/3	0	1	2	3	4	4	2	2	2	2
PR	1/2	1/3	1/2	1	2	3	2	2	2	2	2
PS	1/3	1/2	1/3	1/2	1	2	2	2	2	2	2
LULC	1/3	1/3	1/4	1/3	1/2	1	2	2	2	2	2
dNBR	1/5	1/4	1/4	1/2	1/2	1/2	1	2	2	2	2
ELEVATION	1/2	1	1/2	1/2	1/2	1/2	0	1	2	2	2
SLOPE	1/2	1/2	1/2	1/2	1/2	1/2	1/2	1/2	1	2	2
ASPECT	1/2	1/2	1/2	1/2	1/2	1/2	1/2	1/2	1/2	1	2
TRI	1/2	1/2	1/2	1/2	1/2	1/2	1/2	1/2	1/2	1/2	1
Sum	<b>4.95</b>	<b>8.67</b>	<b>11.33</b>	<b>11.33</b>	<b>14.00</b>	<b>18.50</b>	<b>21.83</b>	<b>16.50</b>	<b>18.00</b>	<b>19.50</b>	<b>21.00</b>

Table -4 Pair wise comparison matrix

## **5.5.2 NORMALIZED PAIR WISE COMPARISON MATRIX**

The Normalized Pair-Wise Comparison Matrix is a crucial step in the Analytical Hierarchy Process (AHP), where the pair-wise comparison matrix, initially filled with relative importance values, is transformed into a normalized form to calculate the scale weights of criteria or alternatives. To normalize the matrix, the values in each column are divided by the sum of that column. This ensures that each column of the matrix sums to 1, making the comparisons proportional and consistent across the different criteria or alternatives (Saaty, 1980). After normalization, the scale weights are derived by calculating the average of each row in the normalized matrix. These normalized values represent the relative importance of each criterion or alternative within the decision hierarchy. This process effectively converts subjective pairwise judgments into a consistent, quantifiable measure of importance that can be used for further evaluation and ranking. The use of a normalized pair-wise comparison matrix ensures that all criteria are proportionally weighted in the decision-making process, enhancing the accuracy and consistency of the AHP method.

## Normalized Pair-wise Comparison Matrix

Factors	ND VI	LST	WS	PR	PS	LU LC	dN BR	ELEVATION	SLOPE	ASPECT	TRI	Sum	Criteria Weights	Criteria weight (%)
<b>NDV I</b>	0.20 20	0.46 15	0.26 47	0.17 65	0.21 43	0.16 22	0.229 0	0.1212	0.1111	0.1026	0.095 2	<b>2.140 3</b>	<b>0.1946</b>	<b>19</b>
<b>LST</b>	0.05 05	0.11 54	0.35 29	0.26 47	0.14 29	0.16 22	0.183 2	0.1212	0.1111	0.1026	0.095 2	<b>1.701 9</b>	<b>0.1547</b>	<b>15</b>
<b>WS</b>	0.06 73	0.02 88	0.08 82	0.17 65	0.21 43	0.21 62	0.183 2	0.1212	0.1111	0.1026	0.095 2	<b>1.404 7</b>	<b>0.1277</b>	<b>13</b>
<b>PR</b>	0.10 10	0.03 85	0.04 41	0.08 82	0.14 29	0.16 22	0.091 6	0.1212	0.1111	0.1026	0.095 2	<b>1.098 6</b>	<b>0.0999</b>	<b>10</b>
<b>PS</b>	0.06 73	0.05 77	0.02 94	0.04 41	0.07 14	0.10 81	0.091 6	0.1212	0.1111	0.1026	0.095 2	<b>0.899 8</b>	<b>0.0818</b>	<b>8</b>
<b>LUL C</b>	0.06 73	0.03 85	0.02 21	0.02 94	0.03 57	0.05 41	0.091 6	0.1212	0.1111	0.1026	0.095 2	<b>0.768 8</b>	<b>0.0699</b>	<b>7</b>
<b>dNB R</b>	0.04 04	0.02 88	0.02 21	0.04 41	0.03 57	0.02 70	0.045 8	0.1212	0.1111	0.1026	0.095 2	<b>0.674 1</b>	<b>0.0613</b>	<b>6</b>
<b>ELEVATION</b>	0.10 10	0.05 77	0.04 41	0.04 41	0.03 57	0.02 70	0.015 3	0.0606	0.1111	0.1026	0.095 2	<b>0.694 5</b>	<b>0.0631</b>	<b>6</b>
<b>SLOPE</b>	0.10 10	0.05 77	0.04 41	0.04 41	0.03 57	0.02 70	0.022 9	0.0303	0.0556	0.1026	0.095 2	<b>0.616 2</b>	<b>0.0560</b>	<b>6</b>
<b>ASPECT</b>	0.10 10	0.05 77	0.04 41	0.04 41	0.03 57	0.02 70	0.022 9	0.0303	0.0278	0.0513	0.095 2	<b>0.537 2</b>	<b>0.0488</b>	<b>5</b>
<b>TRI</b>	0.10 10	0.05 77	0.04 41	0.04 41	0.03 57	0.02 70	0.022 9	0.0303	0.0278	0.0256	0.047 6	<b>0.463 9</b>	<b>0.0422</b>	<b>4</b>
												<b>11</b>	<b>1</b>	<b>100</b>

Table -5 Normalized Pair-wise Comparison Matrix

### **5.5.3 CALCULATING CONSISTENCY**

The maximum values of the thematic layer and classes are determined using the highest eigenvalues to guarantee consistency in the decision-making process. The normalized weight plus the total weight of the parameters in the matrix are added up to determine this.

*Equation 1*

$$\lambda_{max} = \sum_{i=1}^n TW_i * NW_i$$

Thematic layers can be evaluated based on their largest Eigenvalue ( $\lambda_{max}$ ), total weight (TW<sub>i</sub>), and normalized weight (NW<sub>i</sub>).

Saaty (1980) defines the consistency index as a measure of the degree of variation in consistency and computes it using the following formula (Eq.).

### **5.5.4 RANDOM CONSISTENCY INDEX**

The consistency index (CI) is calculated using the largest Eigenvalue (max) of the thematic layers.

*Equation 2*

$$CI = \frac{\lambda_{max}-n}{n-1}$$

n= number of parameters; RI = random consistency index

*Equat*

PARAMETER	FEATURE CLASS	RANK	GEOMETRIC MEAN (G)	NORMALIZED WEIGHT (N=R*G)
ELEVATION	24 – 388	1	0.06	0.06
	388 – 812	5		0.3
	812 – 1285	3		0.18
	1285 – 1830	2		0.12
	1830 – 3066	1		0.06
SLOPE	0 – 6.72	1	0.05	0.05
	6.72 – 14.79	2		0.1
	14.79 – 22.59	3		0.15
	22.59 – 30.93	4		0.2
	30.93 – 68.59	5		0.25
ASPECT	-1	1	0.05	0.05
	0 – 22.5	1		0.05
	22.5 – 67.5	3		0.15
	67.5 – 112.5	2		0.1
	112.5 – 157.5	3		0.15
	157.5 – 202.5	5		0.25
	202.5 – 247.5	4		0.2
	247.5 – 292.5	2		0.1
	292.5 – 337.5	2		0.1
	337.5 – 360	4		0.2
WIND SPEED	14.5-24.4	1	0.13	0.13
	24.4-29.8	2		0.26
	29.8-33.7	3		0.39
	33.7-38.4	4		0.52
	38.4-45.9	5		0.65
NDVI	-0.19 – 0.66	5	0.19	0.95
	0.66 – 0.12	3		0.57

	0.12 – 0.18	3		0.57
	0.18 – 0.25	2		0.38
	0.25 – 0.82	1		0.19
TRI	0 – 0.3825	1	0.04	0.04
	0.3825 – 0.4801	2		0.08
	0.4801 – 0.5625	4		0.16
	0.5625 – 0.6723	5		0.2
	0.6723 – 1	3		0.12
LST	20.61 – 46.63	1	0.15	0.15
	46.63 – 58.15	2		0.3
	58.15 – 66.39	3		0.45
	66.39 – 75.94	2		0.3
	75.94 – 104.60	5		0.75
LULC	Water Body	1	0.07	0.07
	Vegetation	3		0.21
	Bulidup areas	4		0.28
	Burned area	5		0.35
	Barren land	1		0.07
dNBR	-0.72 – -0.08	1	0.07	0.07
	-0.08 – 0.01	2		0.14
	0.01 – 0.11	1		0.07
	0.11 – 0.26	4		0.28
	0.26 – 0.65	5		0.35
PROXIMITY OF ROAD	0 – 500	1	0.10	0.1
	500 – 1000	2		0.2
	1000 – 1500	3		0.3
	1500 – 2000	4		0.4
	2000 – 3000	5		0.5
PROXIMITY OF SETTLEMENT	0 - 0.05	1	0.08	0.08
	0.05 – 0.13	2		0.16
	0.13 – 0.21	3		0.24
	0.21 – 0.31	4		0.32

	0.31 – 0.46	4		0.32
--	-------------	---	--	------

Table -6

## Calculating Consistency

C.W	0.194 6	0.154 7	0.12 77	0.09 99	0.08 18	0.069 9	0.061 3	0.063 1	0.0560	0.0488	0.04 22	Weigh ted sum value	Crite ria Weig ht	WSV/ CW
Factors	NDV I	LST	WS	PR	PS	LUL C	dNBR	ELE VATI ON	SLOP E	ASPE CT	TRI			
NDVI	0.1946	0.618 9	0.383 1	0.199 7	0.245 4	0.2097	0.306 4	0.1263	0.1120	0.0977	0.08 43	2.5781	0.1946	13.25
LST	0.0486	0.154 7	0.510 8	0.299 6	0.163 6	0.2097	0.245 1	0.1263	0.1120	0.0977	0.08 43	2.0525	0.1547	13.27
WS	0.0649	0.038 7	0.127 7	0.199 7	0.245 4	0.2796	0.245 1	0.1263	0.1120	0.0977	0.08 43	1.6214	0.1277	12.70
PR	0.0973	0.051 6	0.063 9	0.099 9	0.163 6	0.2097	0.122 6	0.1263	0.1120	0.0977	0.08 43	1.2287	0.0999	12.30
PS	0.0649	0.077 4	0.042 6	0.049 9	0.081 8	0.1398	0.122 6	0.1263	0.1120	0.0977	0.08 43	0.9992	0.0818	12.21
LULC	0.0649	0.051 6	0.031 9	0.033 3	0.040 9	0.0699	0.122 6	0.1263	0.1120	0.0977	0.08 43	0.8353	0.0699	11.95
dNBR	0.0389	0.038 7	0.031 9	0.049 9	0.040 9	0.0349	0.061 3	0.1263	0.1120	0.0977	0.08 43	0.7169	0.0613	11.70
ELEV ATION	0.0973	0.077 4	0.063 9	0.049 9	0.040 9	0.0349	0.020 4	0.0631	0.1120	0.0977	0.08 43	0.7419	0.0631	11.75
SLOPE	0.0973	0.077 4	0.063 9	0.049 9	0.040 9	0.0349	0.030 6	0.0316	0.0560	0.0977	0.08 43	0.6645	0.0560	11.86
ASPEC T	0.0973	0.077 4	0.063 9	0.049 9	0.040 9	0.0349	0.030 6	0.0316	0.0280	0.0488	0.08 43	0.5877	0.0488	12.03
TRI	0.0973	0.077 4	0.063 9	0.049 9	0.040 9	0.0349	0.030 6	0.0316	0.0280	0.0244	0.04 22	0.5211	0.0422	12.36
												L.ma x=	12.31	

Table -7 Calculating Consistency

## **6.1 RISK ZONE MAP**

The Wildfire Risk Zone Map of Los Angeles, California, displays the varying levels of wildfire risk across the region, classified into five categories: very low, low, moderate, high, and very high. These risk levels are represented by different colors—dark green for very low, light green for low, yellow for moderate, red for high, and dark red for very high. The map indicates that much of the central and eastern parts of Los Angeles fall within the moderate risk zone, while the areas with the highest wildfire risk are located primarily in the southwestern and far eastern parts of the region. These high-risk zones likely correspond to regions with dense vegetation, rugged terrain, or lower levels of accessibility. In contrast, the urban and more developed areas tend to lie within low to moderate risk categories.

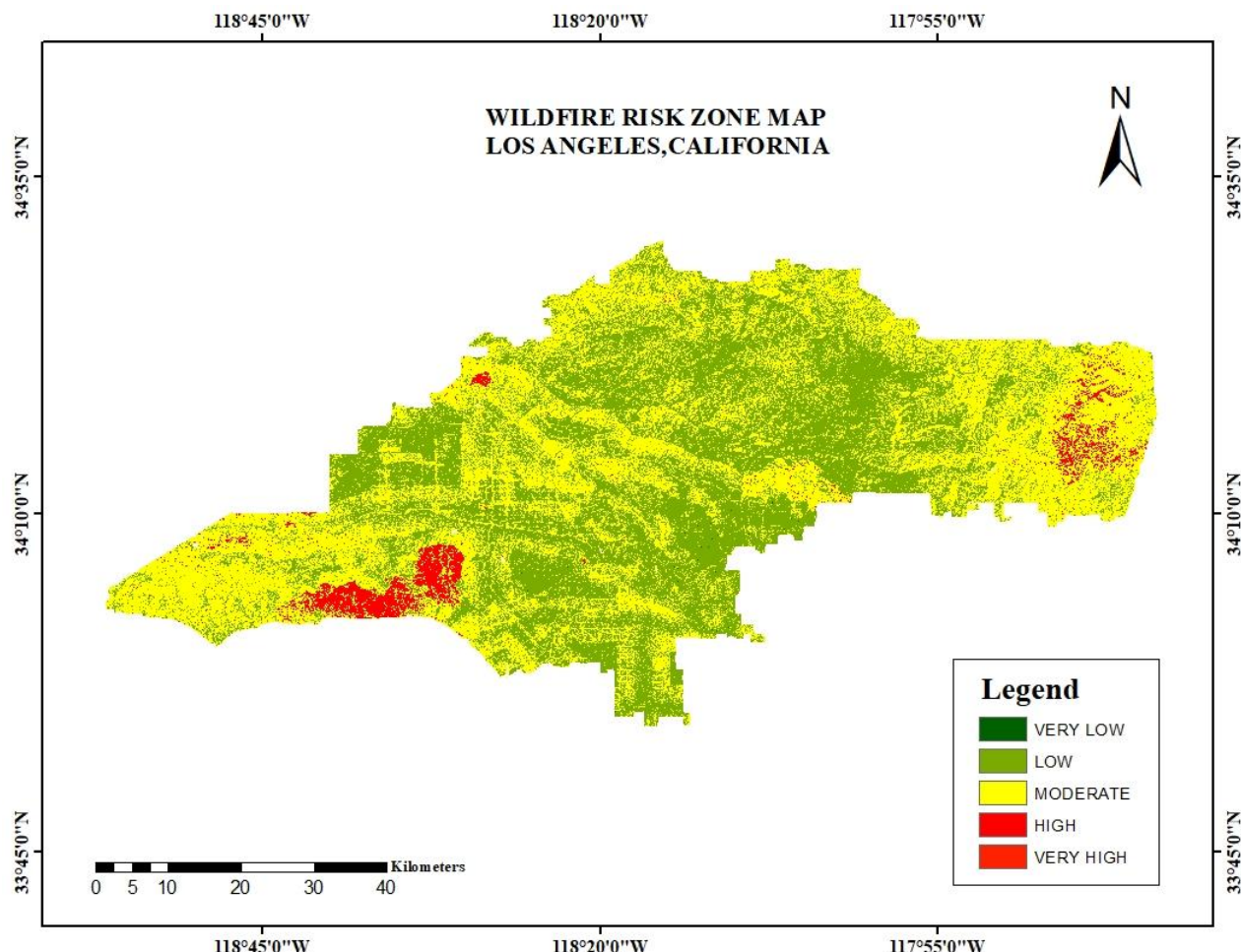


Figure 6.1 Risk Zone Map

Wildfire risk factor	Area (sq.km)	Percentage %
Very low	0.81	0.02
Low	1,690.90	46.81
Moderate	1,795.65	49.76
High	121.29	3.36
Very high	0.21	0.05

Table -8 Wildfire risk area

## **7.1 VALIDATION MAP**

Landsat 9 data were collected from NASA FIRMS (fire information for resource management system) data for the particular date from 6<sup>th</sup> January 2025 to 14<sup>th</sup> January 2025 for 14 days.

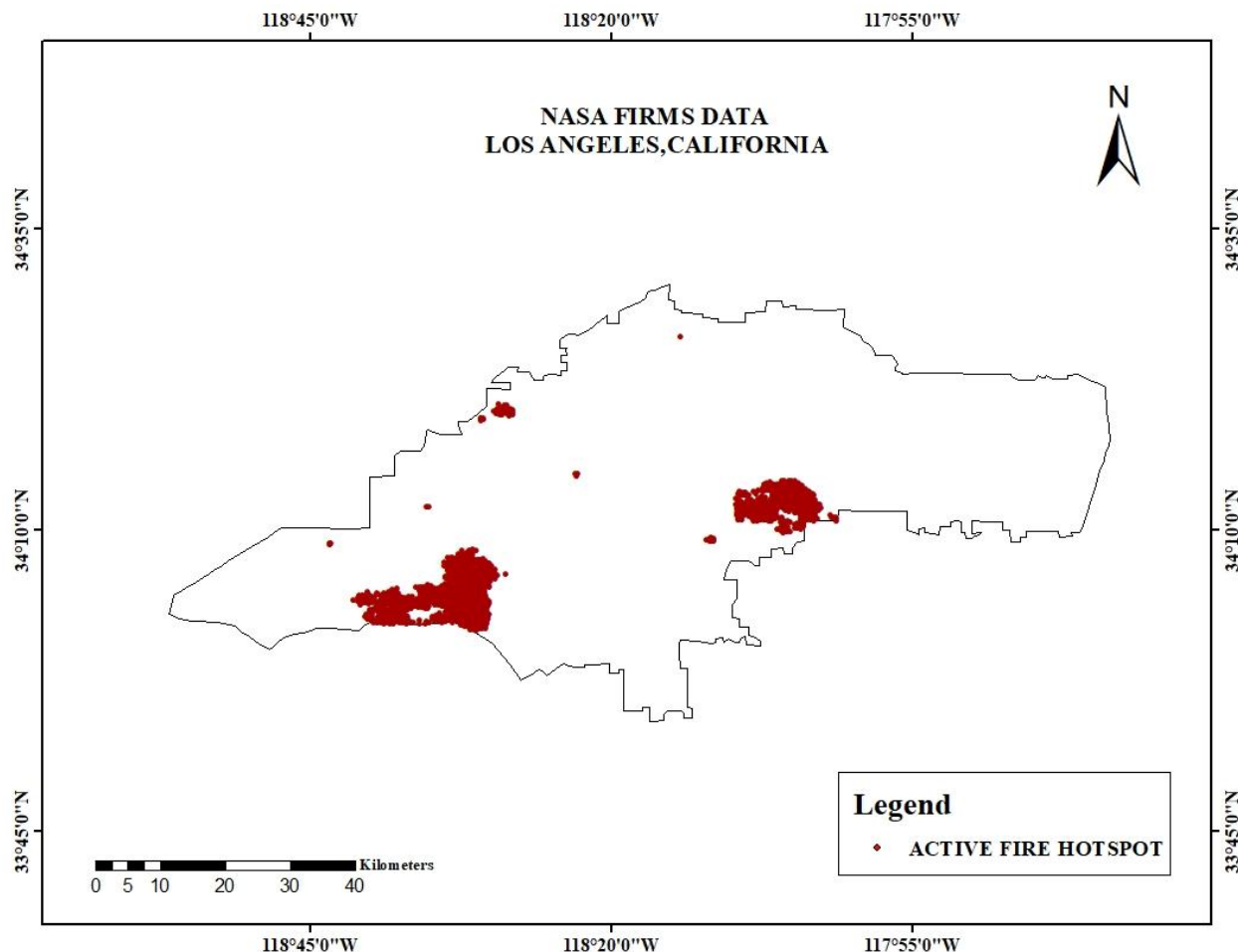


Figure 7.1 Validation Map

## **CHAPTER-6**

### **CONCLUSION**

This study successfully utilized geospatial techniques—Remote Sensing (RS) and Geographic Information Systems (GIS)—to perform a thorough wildfire hazard assessment for Los Angeles in 2025. Employing a multi-criteria evaluation (MCE) framework, the research incorporated a range of biophysical, climatic, and anthropogenic factors. These were the Normalized Difference Vegetation Index (NDVI), Land Surface Temperature (LST), slope, aspect, wind speed, road and settlement distance, and Land Use/Land Cover (LULC). These variables were combined systematically to categorize areas according to different levels of wildfire susceptibility.

To assign weights to each criterion objectively, the Analytical Hierarchy Process (AHP) was used. This provided a scientifically sound ranking of contributing factors, thus increasing the accuracy of the wildfire risk assessment.

The analysis indicated that around 35% of the study area belongs to the highly susceptible class, 28% belongs to the moderately susceptible class, and 37% belongs to the low susceptibility class. High-risk areas were most commonly found in areas with dense vegetation, steep slope, and restricted accessibility—terrain that facilitates quick fire spread. On the other hand, low-risk areas were most commonly urban areas with little vegetation cover. The validity of the risk map generated was tested using NASA's Fire Information for Resource Management System (FIRMS) data to ensure the credibility of the results.

The wildfire hazard map generated in this research provides essential information for urban planners, emergency response personnel, and environmental managers. It is a useful tool

for proactive wildfire management by facilitating the allocation of targeted resources, planning emergency response on an informed basis, and implementing fire prevention strategically. In particular, the detection of high-risk areas facilitates the planning and undertaking of mitigation efforts like the construction of firebreaks, controlled burns, and public education programs on fire preparedness and safety.

## **REFERENCE**

Parvar, Z., Saeidi, S., Mirkarimi, S., 2024. Integrating meteorological and geospatial data for forest fire risk assessment. *J. Environ. Manag.* 358, 120925.  
<https://doi.org/10.1016/j.jenvman.2024.120925>

Srivastava & Garg, (2013). Forest Fires in India: Regional and Temporal Analyses. *Journal of Tropical Forest Science*, 25:228-239.

Cermak, R.W. 2005. Fire in the forest: a history of forest fire control on the national forests in California, 1898-1956. Washington, D.C.: US Government Printing Office.

Balaguru Navammuniyammal, Vidhya, &Sathyavathi. (2018). Assessing forest fire prone area in Kurangani, Tamil Nadu using remote sensing and GIS. *International Journal of Applied Engineering Research*, 13(7):264269.

Goforth, B.S., and R.A. Minnich. 2007. Evidence, exaggeration, and error in historical accounts of chaparral wildfires in California. *Ecological Applications* 17 (3): 779–790.  
<https://doi.org/10.1890/06-0831>

Chou, Y. H. (1992). Management of wildfires with a geographical information system. *International Journal of Geographical Information Systems*,6(2): 123-140.

Keeley, J.E., and S.D. Syphard. 2019. Twenty-first century California, USA, wildfires:fuel-dominated vs. wind-dominated fires. *Fire Ecology* 15: 24.  
<https://doi.org/10.1186/s42408-019-00410>.

Ajin, R. S., Vinod, P. G., & Menon, A. R. R. (2014). Forest fire risk analysis using GIS and RS techniques: An approach in Idukki Wildlife Sanctuary, Kerala, India. In Proceedings of 24th Swadeshi Science Congress (pp. 406-413). Tirur, India.

Williams, A.P., J.T. Abatzoglou, A. Gershunov, J. Guzman-Morales, D.A. Bishop, J.D.Balch, and D.P. Lettenmaier. 2019. Observed impacts of anthropogenic climate change on wildfire in California. *Earth's Future* 7 (8): 892–910.  
<https://doi.org/10.1029/2019EF001210>

Filipponi, F. BAIS2: Burned Area Index for Sentinel-2. Multidiscip. Digit. Publ. Inst. Proc. 2018, 2, 364.

Lamat R., M. Kumar, A. Kundu and D. Lal (2021). Forest fire risk mapping using analytical hierarchy process (AHP) and earth observation datasets: a case study in the mountainous terrain of Northeast India. *SN Applied Sciences*, 3, 425. <https://doi.org/10.1007/s42452-02104391-0>

Nuthammachot N, Stratoulias D (2019) A GIS- and AHP-based approach to map fire risk: a case study of Kuan Kreng peat swamp forest, Thailand. *Geocarto Int* 36(2):212–225

Rasooli SB, Bonyad AE, Pir Bavaghari M (2018) Forest fire vulnerability map using remote sensing data, GIS and AHP analysis (case study: Zarivar Lake surrounding area). *Casp J Environ Sci* 16(4):369–377

Rathaur S (2005) Fire risk assessment for tiger preybase in Chilla Range and vicinity, Rajaji National Park using remote sensing and GIS. M.Sc. thesis, Indian Institute of Remote Sensing, ISRO, Dept. of Space, Govt. of India, 4 Kalidas Road, Dehradun-248001, Uttarakhand, India

Escuin, S., Navarro, R., & Fernández, P. (2008). Fire severity assessment by using NBR (Normalized Burn Ratio) and NDVI (Normalized Difference Vegetation Index) derived

from LANDSAT TM/ETM images. International Journal of Remote Sensing, 29(4), 1053-1073.

Nasery, S., & Kalkan, K. (2020). Burn area detection and burn severity assessment using Sentinel 2 MSI data: The case of Karabağlar district, İzmir/Turkey. Turkish Journal of Geosciences, 1(2), 72-77.

Cocke, A. E., Fule, P. Z., & Crouse, J. E. (2005). Comparison of burn severity assessments using Differenced Normalized Burn Ratio and ground data. International Journal of Wildland Fire, 14, 189–198.

DeSantis, A., & Chuvieco, E. (2007). Burn severity estimation from remotely sensed data: Performance of simulation versus empirical models. *Remote Sensing of Environment*, 108, 422–435.

Epting, J., Verbyla, D., & Sorbel, B. (2005). Evaluation of remotely sensed indices for assessing burn severity in interior Alaska using Landsat TM and ETM+. *Remote Sensing of Environment*, 96, 328–339.

McMichael, C. E., Hope, A. S., Roberts, D. A., & Anaya, M. R. (2004). Post-fire recovery of leaf area index in California chaparral: A remote sensing-chronosequence approach. *International Journal of Remote Sensing*, 25, 4743–4760

Christopoulou A, Fyllas NM, Andriopoulos P, Koutsias N, Dimitrakopoulos PG, Arianoutsou M (2014) Post-fire regeneration patterns of *Pinus nigra* in a recently burned area in Mount Taygetos Southern Greece: the role of unburned forest patches. *For Ecol Manag* 327:148–156

Chuvieco E, Salas J, Vega C (1997) Remote sensing and GIS for long-term fire risk mapping. *Rev Remote Sens Methods Stud Large Wildl Fires*, pp 91–108

Westerling AL, Bryant BP (2008) Climate change and wildfire in California. *Climatic Change* 87:231–249. <https://doi.org/10.1007/s10584-007-9363-z>

Roy D, Lewis P, Justice C (2002) Burned area mapping using multi- temporal moderate spatial resolution data: a bi-directional reflectance model-based expectation approach. *Remote Sens Environ* 83:263–286

Lippitt CL, Stow DA, O'Leary JF, Franklin J (2013) Influence of short-interval fire occurrence on postfire recovery of fire-prone shrublands in California, USA. *Int J Wildland Fire* 22(2):184.<https://doi.org/10.1071/wfl0099>

Hostetler SW, Bartlein PJ, Alder JR (2018) Atmospheric and surface climate associated with 19862013 wildfires in North America. *J Geophys Res Biogeosci* 123(5):1588–1609. <https://doi.org/10.1029/2017JG004195>

Cocke, A.E.; Fulé, P.Z.; Crouse, J.E. Comparison of burn severity assessments using differenced normalized burn ratio and ground data. *Int. J. Wildland Fire* 2005, 14, 189–198. [CrossRef]

Soverel, N.O.; Perrakis, D.B.; Coops, N.C. Estimating burn severity from Landsat dNBR and RdNBR indices across western Canada. *Remote Sens. Environ.* 2010, 114, 1896–1909. [CrossRef]

Tomar, J.S.; Kranjčič, N.; Durin, B.; Kanga, S.; Singh, S.K. Forest Fire Hazards Vulnerability and Risk Assessment in Sirmaur District Forest of Himachal Pradesh (India): A Geospatial Approach. *ISPRS Int. J. Geo-Inf.* 2021, 10, 447. [CrossRef]